

## Two Substrate Sites in the Renal Na<sup>+</sup>-D-Glucose Cotransporter Studied by Model Analysis of Phlorizin Binding and D-Glucose Transport Measurements

Hermann Koepsell, Günter Fritzsich, Klaus Korn, and Andrzej Madrala

Max-Planck-Institut für Biophysik, 6000 Frankfurt (Main) 70, Federal Republic of Germany

**Summary.** Time courses of phlorizin binding to the outside of membrane vesicles from porcine renal outer cortex and outer medulla were measured and the obtained families of binding curves were fitted to different binding models. To fit the experimental data a model with two binding sites was required. Optimal fits were obtained if a ratio of low and high affinity phlorizin binding sites of 1:1 was assumed. Na<sup>+</sup> increased the affinity of both binding sites. By an inside-negative membrane potential the affinity of the high affinity binding site (measured in the presence of 3 mM Na<sup>+</sup>) and of the low affinity binding site (measured in the presence of 3 or 90 mM Na<sup>+</sup>) was increased. Optimal fits were obtained when the rate constants of dissociation were not changed by the membrane potential. In the presence of 90 mM Na<sup>+</sup> on both membrane sides and with a clamped membrane potential,  $K_D$  values of 0.4 and 7.9  $\mu$ M were calculated for the low and high affinity phlorizin binding sites which were observed in outer cortex and in outer medulla. Apparent low and high affinity transport sites were detected by measuring the substrate dependence of D-glucose uptake in membrane vesicles from outer cortex and outer medulla which is stimulated by an initial gradient of 90 mM Na<sup>+</sup> (out > in). Low and high affinity transport could be fitted with identical  $K_m$  values in outer cortex and outer medulla. An inside-negative membrane potential decreased the apparent  $K_m$  of high affinity transport whereas the apparent  $K_m$  of low affinity transport was not changed. The data show that in outer cortex and outer medulla of pig high and low affinity Na<sup>+</sup>-D-glucose cotransporters are present which contain low and high affinity phlorizin binding sites, respectively. It has to be elucidated from future experiments whether equal amounts of low and high affinity transporters are expressed in both kidney regions or whether the low and high affinity transporter are parts of the same glucose transport molecule.

**Key Words** coupled transport · glucose transport · substrate sites · brush-border membrane · proximal tubule · vesicles · phlorizin binding

### Introduction

In the last few years knowledge concerning the Na<sup>+</sup>-D-glucose cotransporter has rapidly increased. For Na<sup>+</sup>-D-glucose cotransport in calf kidney a functional molecular weight of 345,000, and for

phlorizin binding in rabbit kidney functional molecular weights of 230,000 and 110,000 have been determined by target size analysis [23, 31, 34]. With amino acid specific reagents a  $M_r$  75,000 polypeptide has been identified as a component of the intestinal transporter in rabbit [27, 28] and with covalently binding D-glucose analogs and monoclonal antibodies [10, 18, 25, 26]  $M_r$  75,000 and 47,000 polypeptides have been shown to be components of the renal transporter in pig and rat. Furthermore, a cDNA coding for a  $M_r$  73,080 polypeptide was cloned from rabbit intestine which was able to drastically increase Na<sup>+</sup>-D-glucose cotransport in oocytes from *Xenopus laevis* after injection of the corresponding mRNA [12]. It has been shown that the renal and intestinal Na<sup>+</sup>-D-glucose cotransporters are asymmetric proteins, since Na<sup>+</sup> stimulation was only observed for D-glucose uptake from the luminal to the intracellular side of the membrane [14, 19] and since only from the luminal side could Na<sup>+</sup>-dependent D-glucose uptake be inhibited by phlorizin [19]. In membrane vesicles from outer cortex of rabbit kidneys low affinity D-glucose transport with high capacity and a Na<sup>+</sup>/D-glucose stoichiometry of 1:1 [36, 37] and in membrane vesicles from outer medulla high affinity D-glucose transport with a Na<sup>+</sup>/D-glucose stoichiometry of 2:1 has been described [35]. However, both high and low affinity Na<sup>+</sup>-D-glucose cotransport has been recently detected in outer cortex of rat kidneys [3]. In intestine high and low affinity transport with different sensitivities to changes in temperature have also been described [4]. In a recent paper [38] it has been reported that oocytes from *Xenopus laevis* exhibit varying degrees of endogeneous activities of high plus low affinity Na<sup>+</sup>-D-glucose cotransport.

The large functional molecular weights of phlorizin binding and D-glucose transport in kidney which were estimated by target size analysis [23, 31, 34] may be explained by the assumption that the

transporter is an oligomer consisting of  $M_r$  75,000 and/or  $M_r$  47,000 polypeptides. The differences in the functional molecular weight of phlorizin binding and D-glucose transport suggest that the functional unit of transport consists of more polypeptides than those involved in phlorizin binding. Since in purification attempts a correlation between enrichment of reconstituted Na<sup>+</sup>-D-glucose cotransport and Na<sup>+</sup>-dependent high affinity phlorizin binding was not observed [16, 17], the question was asked whether or not the Na<sup>+</sup>-D-glucose cotransporter may exist in a nontransporting state in which phlorizin can bind. It was not clear whether the methods used to analyze the number of phlorizin binding sites and  $V_{max}$  of D-glucose transport detected all the transporter molecules. Furthermore, since the characteristics for substrate dependence of Na<sup>+</sup>-D-glucose cotransport measured after reconstitution of the transporter from renal cortex were similar to those observed in membrane vesicles from outer medulla (H. Koepsell, *unpublished data*) we wondered if different functional states of the same transporter exist in outer cortex and outer medulla.

In the present study we have tried to fit families of onset curves of phlorizin binding at membrane vesicles from outer renal cortex and outer medulla with different models. In addition we have attempted to fit measurements of D-glucose transport at different D-glucose concentrations with models in which one or two transport sites are assumed. We could demonstrate that the Na<sup>+</sup>-D-glucose cotransporter contains two coexisting Na<sup>+</sup>-dependent phlorizin binding sites which are present at a stoichiometry of 1:1. Our data suggest that both types of phlorizin binding sites are equivalent to D-glucose transport sites. The data are consistent with the hypotheses (i) that two substrate sites are present on one functional transporter, (ii) that the Na<sup>+</sup>-D-glucose cotransporters in outer cortex and outer medulla are identical, and (iii) that functional differences of transport in outer cortex and outer medulla which are observed under certain experimental conditions are due to different microenvironments of the transporter.

## Materials and Methods

### METHODS

#### *Isolation of Brush-Border Membrane Vesicles*

Porcine kidneys were obtained immediately after slaughter and the outermost 2 mm of the cortex was dissected. To obtain tissue from the outer medulla the white "inner medulla" and the red "inner stripe of the outer medulla" were carefully removed from the same kidneys and about 3 mm of the "outer stripe of the

outer medulla" were dissected [22]. From both kidney regions brush-border membrane vesicles were isolated by differential centrifugation in the presence of Ca<sup>2+</sup>, suspended in 10 mM triethanolamine-HCl, pH 7.4, 150 mM NaCl, 5 mM EDTA disodium salt, 10% (vol/vol) glycerol and frozen in liquid nitrogen in 1-ml portions [21]. For binding and transport measurements 1-ml portions of vesicles were thawed at 37°C, suspended in 20 ml (22°C) of 20 mM imidazole cyclamate, pH 7.4, 0.1 mM magnesium cyclamate, 100 mM potassium cyclamate (KC buffer) or of 20 mM imidazole cyclamate, pH 7.4, 0.1 mM magnesium cyclamate, 90 mM sodium cyclamate, 50 mM potassium cyclamate (NaKC buffer), spun down by 20-min centrifugation at 48,000 × *g* (22°C) and washed twice by suspending in 20 ml of KC buffer or NaKC buffer (22°C) and centrifuging for 20 min at 48,000 × *g*.

#### *Measurement of Equilibrium Binding of Phlorizin in the Presence of Na<sup>+</sup> or K<sup>+</sup>*

The measurements were performed with membrane vesicles at a concentration of 6 to 10 mg of protein per ml. Before the measurements the vesicles which contained NaKC buffer (Fig. 1a) or KC buffer (Figs. 1b and 2) were incubated for 5 min at 30°C in the presence (Fig. 1a) or absence (Figs. 1b and 2) of 20 μg valinomycin per ml. For binding measurements 90 μl of incubation buffer (30°C), which contained NaKC buffer (Fig. 1a), KC buffer (Fig. 1b) or 20 mM imidazole cyclamate, pH 7.4, 0.1 mM magnesium cyclamate, 100 mM sodium cyclamate (NaC buffer) (Fig. 2) and in addition 0.05 μM (<sup>3</sup>H)phlorizin or 0.05 μM (<sup>3</sup>H)phlorizin plus different concentrations of nonlabeled phlorizin, was added to 10 μl of membrane vesicles (30°C). After the membrane vesicles were incubated for 10 min at 30°C with (<sup>3</sup>H)phlorizin in the presence of Na<sup>+</sup> and/or K<sup>+</sup> the reaction was stopped by the addition of 1 ml of ice-cold NaKC buffer (Fig. 1a) or NaC buffer (Figs. 1b and 2). Then the sample was applied to 0.22-μm cellulose acetate filters (Millipore GSWP), washed with 5 ml of the respective ice-cold stop solution and the radioactivity on the filters was measured [20]. The binding measurements in the presence of Na<sup>+</sup> and K<sup>+</sup> were corrected for nonspecific phlorizin binding: First, (<sup>3</sup>H)phlorizin binding measured in the presence of 5 mM nonlabeled phlorizin was subtracted.<sup>1</sup> Second, a fraction of nonspecific (<sup>3</sup>H)phlorizin binding was subtracted which was not removed by 5 mM cold phlorizin. For the measurements performed in the presence of 90 mM Na<sup>+</sup> (Figs. 1a and 2) this fraction of nonspecific phlorizin binding was calculated from measurements in which the linear nonsaturable increase of phlorizin binding, which could not be suppressed by the addition of 5 mM nonlabeled phlorizin, was measured in the range of phlorizin concentrations between 50 to 200 μM. The amount of this nonspecific phlorizin binding related to amount of membrane protein and phlorizin concentration was  $5.33 \pm 0.23 \text{ pmol} \cdot (\text{mg of protein})^{-1} \cdot \mu\text{M}^{-1}$ .<sup>2</sup> In phlorizin binding measurements performed in the absence of Na<sup>+</sup> (Fig. 1b) this second fraction of nonspecific

<sup>1</sup> For the measurements of equilibrium binding in the presence of Na<sup>+</sup> or K<sup>+</sup> (performed with phlorizin concentrations between 0.04 and 100 μM) this fraction of nonspecific phlorizin binding amounted to between 2 and 50% of the total phlorizin binding measured.

<sup>2</sup> In the equilibrium binding measurements reported in this paper (performed with phlorizin concentrations between 0.04 to 100 μM) this fraction of nonspecific phlorizin binding amounted to between 2 and 30% of the total phlorizin binding measured.

phlorizin binding could not be determined.<sup>3</sup> It was therefore assumed to be the same as in the presence of Na<sup>+</sup>. In Figs. 1 and 2 representative examples of three independent experiments are shown.

### Measurement of the Onset of Phlorizin Binding

Membrane vesicles, at a concentration of 4 to 10 mg of protein per ml, which were preloaded with NaKC buffer (Fig. 3), with 20 mM imidazole cyclamate, pH 7.4, 0.1 mM magnesium cyclamate, 97 mM potassium cyclamate plus 3 mM sodium cyclamate (Figs. 4 and 8), or with KC buffer (Figs. 6, 7 and 9) were incubated for 10 min at 30°C in the absence and presence of 20 µg valinomycin per ml. Membrane vesicles (10 µl) were incubated at 30°C with 90 µl of 20 mM imidazole cyclamate, pH 7.4, 0.1 mM magnesium cyclamate containing different concentrations of sodium cyclamate and potassium cyclamate plus different concentrations of (<sup>3</sup>H)phlorizin. After time intervals of 2 to 60 sec or after 10 min, 1 ml of ice-cold NaKC buffer (Fig. 3) or NaC buffer (Figs. 4 and 6–9) was added and the samples were applied to filters, washed with the respective stop solutions and analyzed for radioactivity as described for equilibrium binding measurements. Phlorizin binding after the very beginning of incubation was measured by adding the membrane vesicles and the incubation buffer directly to the stop solution.<sup>4</sup> In principle, phlorizin binding in the presence of 90 or 3 mM Na<sup>+</sup> was corrected for nonspecific phlorizin binding as described in the equilibrium binding measurements: First, a phlorizin binding measured in the presence of 5 mM nonlabeled phlorizin was subtracted<sup>5</sup> and second, a fraction of nonspecific phlorizin binding was subtracted which could not be removed by the addition of 5 mM nonlabeled phlorizin. This latter fraction of nonspecific binding was calculated from the linear increase of phlorizin binding which was observed after the nonspecific phlorizin measured in the presence of 5 mM nonlabeled phlorizin had been subtracted.<sup>6</sup> Since the second fraction of nonspecific binding increased with time it was calculated separately for the different times of phlorizin incubation used in the experiments.<sup>7</sup> In Figs. 3, 4 and 6–9 the corrected amount of

phlorizin binding is indicated by *b*. The binding measurements obtained after 10-min incubation were plotted according to Scatchard and the total number of phlorizin binding sites (*n*) was determined by linear regression analysis from the low affinity branches of the curvilinear Scatchard plots and by fitting the data with a two-site model. The results obtained by both methods were not significantly different. In Figs. 3, 4 and 6–9 the data on the onset of phlorizin binding were presented as the fraction of nonoccupied phlorizin binding sites (*n* – *b*)/*n* after different time intervals of incubation. In Figs. 3, 4 and 6–9 representative examples of two or three independent experiments are presented.

### Measurement of D-Glucose Uptake in the Presence of a Na<sup>+</sup>-Gradient

Initial D-glucose uptake rates into membrane vesicles were measured in the presence of an initial concentration gradient of 90 mM Na<sup>+</sup> (out > in) and corrected for nonspecific glucose uptake which was determined by measuring uptake of L-glucose at K<sup>+</sup> equilibrium. The measurements were performed at 30 or 37°C. To measure D-glucose uptake 10 µl of membrane vesicles containing KC buffer were added to 90 µl of NaC which contained different concentrations of (<sup>3</sup>H)D-glucose. Nonspecific uptake was measured by adding 10 µl of membrane vesicles containing KC buffer to 90 µl of KC buffer containing the respective concentrations of (<sup>3</sup>H)L-glucose. After 2-sec incubation of the vesicles with (<sup>3</sup>H)D-glucose or (<sup>3</sup>H)L-glucose the reaction was stopped by adding 1 ml of ice-cold NaC or KC buffer, respectively. Then the samples were applied to a 0.22-µm cellulose acetate filter (Millipore GSWP), washed with 5 ml of the respective ice-cold stop solution and the radioactivity on the filters was measured [20]. D-glucose uptake at time 0, which was measured by adding the membrane vesicles and the incubation media to the respective ice-cold stop solutions, was at maximum 10% of the uptake measured after 2-sec incubation in the presence of Na<sup>+</sup>. The D-glucose uptake rates were calculated by subtracting the uptake rates of D-glucose in the presence of the inwardly directed Na<sup>+</sup> gradient from those of L-glucose measured at K<sup>+</sup> equilibrium. In Figs. 10 and 11 representative examples of three independent experiments are shown.

### Analysis of Time Courses of Phlorizin Binding

The nine families of experimental curves presented in Figs. 3, 4 and 6–9 were fitted to the time courses of the following six putative reaction schemes (Eqs. (1–6)) of phlorizin binding. In these *E*, *E*<sub>1</sub> and *E*<sub>2</sub> represent phlorizin binding sites which are accessible for phlorizin; *E*\* is a phlorizin binding site that is not accessible for phlorizin added to the outside of the membrane vesicles; *S* indicates phlorizin; *E* · *S*, *E*<sub>1</sub> · *S*, *E*<sub>1</sub> : *S* and *E*<sub>2</sub> · *S* represent transporter-phlorizin complexes at the respective binding sites. In *E* · *S*, *E*<sub>1</sub> · *S* and *E*<sub>2</sub> · *S* phlorizin is bound to one attachment point; in *E* : *S* and *E*<sub>1</sub> : *S* phlorizin is bound to two attachment points.

One site:



two states, one site:



<sup>3</sup> This is because the presumed low affinity phlorizin binding site is supposed to have a very low affinity in the absence of Na<sup>+</sup>, and intolerable high standard deviations were observed in phlorizin binding measurements performed with phlorizin concentrations larger than 600 µM.

<sup>4</sup> These data showed that the amount of phlorizin binding which may occur during blocking and washing was always less than 1% of the measured binding.

<sup>5</sup> For the onset measurements of phlorizin binding (performed in the presence of 90 or 3 mM Na<sup>+</sup> with phlorizin concentrations between 0.04 and 20 µM) this fraction of nonspecific phlorizin binding amounted to between 2 and 25% of the total phlorizin binding measured.

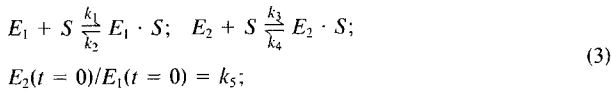
<sup>6</sup> In measurements performed in the presence of 90 or 3 mM Na<sup>+</sup> this fraction of nonspecific phlorizin binding was identical. For measurements at 90 and 3 mM Na<sup>+</sup> it was determined from the linear increase of phlorizin binding measured at phlorizin concentrations between 50 and 200 µM or between 400 and 600 µM, respectively.

<sup>7</sup> For the onset measurements this fraction of nonspecific binding amounted to between 0.2 and 12% of the total phlorizin binding measured.

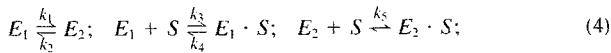
**Table 1.** Eigenvalues and amplitudes of the time courses for models (1) to (6)

	$\mu_{1,2}$	$A_0$
(1) One site	$\mu_1 = -(k_1S_0 + k_2)$ (monophasic)	$\frac{k_2}{k_1S_0 + k_2}$
(2) Two states, one site	$\mu_{1,2} = -\frac{u}{2} \pm \sqrt{\frac{u^2}{4} - k_2k_3S_0 - k_2k_4 - k_1k_4}$ where $u = k_1 + k_2 + k_3S_0 + k_4$	$\frac{(k_1 + k_2)k_4}{\mu_1 \cdot \mu_2}$
(3) Two independent sites	$\mu_1 = -(k_1S_0 + k_2)$ $\mu_2 = -(k_3S_0 + k_4)$	$\frac{1}{1 + k_5} \left( \frac{k_2}{k_1S_0 + k_2} + \frac{k_3k_4}{k_3S_0 + k_4} \right)$
(4) Two dependent sites	$\mu_{1,2} = -\frac{z}{2} \pm \sqrt{\frac{z^2}{4} - k_4 \left( k_1 + \frac{k_2}{1 + k_5S_0} \right) - \frac{k_2k_3S_0}{1 + k_5S_0}}$ where $z = k_1 + \frac{k_2}{1 + k_5S_0} + k_3S_0 + k_4$	$\frac{(k_1 + k_2)^2 \cdot k_4}{\left( \frac{k_2}{1 + k_5S_0} + k_1 \right) \mu_1 \mu_2}$
(5) One site, two-step binding	$\mu_{1,2} = -\frac{v}{2} \pm \sqrt{\frac{v^2}{4} - (k_3 + k_4)k_1S_0 - k_4k_2}$ where $v = k_1S_0 + k_2 + k_3 + k_4$	$\frac{k_4(k_1S_0 + k_2)}{(k_3 + k_4)k_1S_0 + k_4k_2}$
(6) Two independent sites, two-step binding	$\mu_1 = -(w + k_3)$ $\mu_2 = -(k_4S_0 + k_5)$ where $w = \frac{k_1k_2S_0}{1 + k_1S_0}$	$\frac{1}{1 + k_6} \left( \frac{k_3}{w + k_3} + \frac{k_5k_6}{k_4S_0 + k_5} \right)$

two independent sites:



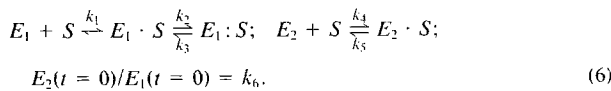
Two dependent sites:



one site, two-step binding:



two independent sites, two-step binding:



Since semilogarithmic plots of our experimental data showed biphasic behavior, the considered reaction models were set up not to require more than two exponential terms. To achieve this for the "two dependent sites model" and for the "two independent sites, two-step binding model" a quasisteady-state assumption had to be made for one reversible reaction step

(see  $k_5$  in Eq. (4) and  $k_1$  in Eq. (6)). For the six reaction schemes the differential equations according to the mass action law were solved analytically. Thereby the concentration of phlorizin ( $S$ ) was assumed to be constant. This assumption was justified since phlorizin was applied in sufficiently high concentrations<sup>8</sup> so that the phlorizin concentration could be regarded as independent of time. Therefore, the kinetic equations of all tested models were of first order. For the best fitting model ("two independent sites, two-step binding," see Eq. (6)) the following equations were derived.

The first step of the reaction is assumed to be very fast (quasisteady state), therefore the quantity  $c = E_1 + E_1 \cdot S$  can be considered as a useful variable and it follows:  $E_1 = c/(1 + k_1S_0)$  and  $E_1 \cdot S = k_1S_0c/(1 + k_1S_0)$ . Here,  $S_0$  stands for the time-independent concentration of phlorizin. This concentration was high enough to be regarded as constant,  $S(t) = S_0$ . Two equations are obtained:

$$\frac{dc}{dt} = -(k_2 + k_3)c + k_5e_{10} \quad (7)$$

$$\frac{dE_2}{dt} = -(k_4S_0 + k_5)E_2 + k_5k_6e_{10} \quad (8)$$

<sup>8</sup> The excess of phlorizin in the incubation buffer over the amount of phlorizin bound to the membrane was usually 100-fold or more. Caused by phlorizin binding to membrane vesicles the phlorizin concentrations were maximally reduced by 5% during the binding measurements.

**Table 1.** *Continued*

A <sub>1</sub>	A <sub>2</sub>
$\frac{k_1 S_0}{k_1 S_0 + k_2}$	0 (monophasic)
$\frac{\mu_1 + k_1 + k_2 + k_4 + \frac{(k_1 + k_2)k_4}{\mu_1}}{\mu_1 - \mu_2}$	$-\left(\frac{\mu_2 + k_1 + k_2 + k_4 + \frac{(k_1 + k_2)k_4}{\mu_2}}{\mu_1 - \mu_2}\right)$
$\frac{1}{1 + k_5} \cdot \frac{k_1 S_0}{k_1 S_0 + k_2}$	$\frac{1}{1 + k_5} \cdot \frac{k_5 k_3 S_0}{k_3 S_0 + k_4}$
$\frac{A_0 \mu_2 + \mu_1 + y}{\mu_1 - \mu_2}$	$-\left(\frac{A_0 \mu_1 + \mu_2 + y}{\mu_1 - \mu_2}\right)$
where	
$y = \frac{(k_1 + k_2) \left( k_1 + k_2 + \frac{k_2 k_4}{1 + k_5 S_0} \right) + k_1 \left( k_3 S_0 + \frac{k_2}{1 + k_5 S_0} \right)}{\frac{k_2}{1 + k_5 S_0} + k_1}$	
$\frac{-\mu_2 + k_4 \frac{k_2 + k_1 S_0}{\mu_1}}{\mu_1 - \mu_2}$	$\frac{\mu_1 - k_4 \frac{k_2 + k_1 S_0}{\mu_2}}{\mu_1 - \mu_2}$
$\frac{w}{(1 + k_6)(w + k_3)}$	$\frac{k_6 k_4 S_0}{(1 + k_6)(k_4 S_0 + k_5)}$

$e_{10}$  is the concentration of  $E_1$  at  $t = 0$ , the concentration of  $E_2$  at  $t = 0$  equals  $k_6 e_{10}$ . The conservation of the total enzyme concentration is included in Eqs. (7) and (8). The solutions of  $c$  and  $E_2$  are of the form

$$f(t) = A_0 + A_1 e^{\mu_1 t} + A_2 e^{\mu_2 t}. \quad (9)$$

The amplitudes  $A_0$ ,  $A_1$  and  $A_2$  and the eigenvalues (exponents)  $\mu_1$  and  $\mu_2$  are functions of the kinetic constants  $k_1, \dots, k_6$ . The functions of amplitudes ( $A_i$ ) and eigenvalues ( $\mu_{1,2}$ ), which were obtained for the six models tested in the paper, are presented in Table 1.

In order to fit the experimental data with the tested reaction models, a nonlinear least-squares curve fitting routine was employed. All curves of a family of time courses were considered in one fit. The experimental data have been weighted according to the reciprocals of their standard errors. Each point is the mean of three measurements. It is assumed that large standard errors bear large uncertainties which are considered with low weights. The curve fitting routine utilized a steepest-descent technique which had been applied for analyses of enzyme inactivation [8, 9]. By means of the initial and the improved estimates a vector of descent is constructed in the parameter space. By a repeated application of this procedure the minimum of the sum of squares is found. Since the iteration described a zig-zag pathway in the parameter space and yielded unstable convergence, a zig-zag prevention was invoked. This was achieved by a built-in memory in the curve fitting routine which averaged the zig-zag

trajectory over a few iteration steps and constructed a new effective vector of descent. The criteria for good models are: (i) Low values of the goodness parameter  $Q^2 = s^2/(k - p)$ , where  $s^2$  is the sum of the least squares,  $k$  the number of experimental data points and  $p$  the number of fitted parameters [24].  $Q^2$  includes not only the least-squares sum but also the number of experimental data and the number of fitted parameters; it allows a qualitative comparison of the models even if they assume different numbers of parameters to be fitted. (ii) Similar values of  $Q^2$  and experimental variance ( $Q^2$  smaller than the experimental variance, i.e., over-determined models did not occur); (iii) Mean residuals (differences between experimental data and corresponding fitted values) approach a Gaussian distribution; (iv) Only weak correlation of residuals (i.e., not too many neighbored experimental points lie on one side of the fitted curve); and (v) stable convergence of roughly good initial estimates.

### *Analysis of Concentration Dependent Phlorizin Equilibrium Binding and D-Glucose Uptake*

Data on phlorizin equilibrium binding (Fig. 1a) and on D-glucose uptake (Figs. 10 and 11) were represented according to Scatchard [29] or Hofstee [13], respectively. In these representations the experimental points are weighted evenly and deviations from linearity which may occur, if, e.g., different transport or binding sites exist, may be detected easily. The data obtained at different experimental conditions (30°C, absence of valinomycin; 37°C,

absence of valinomycin; 37°C, presence of valinomycin) were analyzed by assuming two independent types of phlorizin binding or D-glucose transport sites. The corresponding equation reads:

$$\frac{S_b}{S_f} = \frac{n_{01}}{K_1 + S_f} + \frac{n_{02}}{K_2 + S_f} \quad (10)$$

The meanings of the symbols, which in the following are given without and with parenthesis for phlorizin binding or D-glucose transport measurements, respectively, are:  $S_f$ , concentration of free phlorizin (concentration of free D-glucose);  $S_b$ , measured concentration of bound phlorizin (measured  $V_{\max}$  of D-glucose uptake rate);  $K_1$  and  $K_2$ , dissociation constants of the phlorizin binding sites type 1 and 2 (Michaelis-Menten constant of D-glucose transport at sites 1 and 2);  $n_{01}$  and  $n_{02}$ , total number of phlorizin binding sites type 1 and 2 ( $V_{\max}$  at D-glucose transport site type 1 and 2).

The four constants  $K_1$ ,  $K_2$ ,  $n_{01}$  and  $n_{02}$  were estimated by employing the curve fitting routine described above. The data were weighted according to their experimental error.

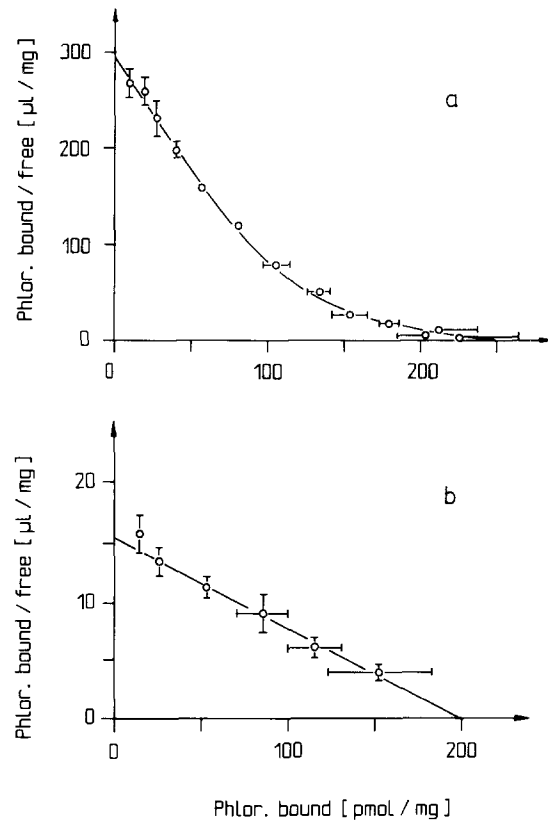
## MATERIALS

D-(<sup>3</sup>H)glucose (33 Ci/mmol), L-(<sup>3</sup>H)glucose (11 Ci/mmol) and (<sup>3</sup>H)phlorizin (55 Ci/mmol) were obtained from New England Nuclear (Dreieich, FRG). Tetra(<sup>3</sup>H)phenylphosphonium bromide (26 Ci/mmol) was supplied by Amersham Buchler (Braunschweig, FRG) and diethylthiadicarbocyanine iodide by Eastman Kodak (Rochester, NY). Phlorizin was purchased from Roth GmbH (Karlsruhe, FRG) and valinomycin from Boehringer GmbH (Mannheim, FRG). All other chemicals were of highest grade and were supplied as described earlier [20].

## Results

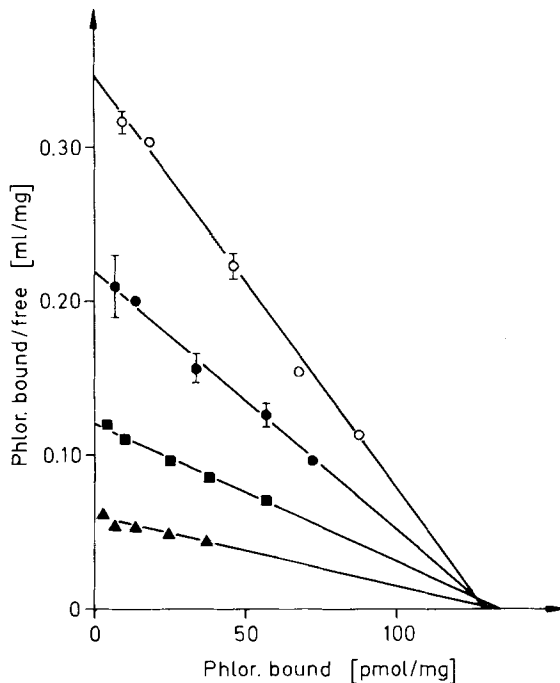
### EQUILIBRIUM BINDING OF PHLORIZIN IN THE PRESENCE OF Na<sup>+</sup> OR K<sup>+</sup>

Membrane vesicles were prepared from the outermost 2 mm of porcine renal cortex and loaded with 90 mM Na<sup>+</sup> plus 50 mM K<sup>+</sup> (Fig. 1a) or with 100 mM K<sup>+</sup> (Fig. 1b). Phlorizin binding was measured when the vesicles were incubated (10 min, 30°C) with different phlorizin concentrations in the presence of valinomycin plus 90 mM Na<sup>+</sup> and 50 mM K<sup>+</sup> (Fig. 1a) or in the presence of 100 mM K<sup>+</sup> (Fig. 1b). In the presence of 90 mM Na<sup>+</sup> plus 50 mM K<sup>+</sup> a curvilinear Scatchard plot was obtained (Fig. 1a) and the binding measurements could be fitted to a model, in which two phlorizin binding sites are assumed (Fig. 1a). For the total number of phlorizin binding sites and for the ratio between low and high affinity phlorizin binding sites respective values of  $238 \pm 9$  pmol · (mg of protein)<sup>-1</sup> and  $1.23 \pm 0.06$  were calculated.  $K_D$ -values of  $0.42 \pm 0.01$  and  $7.91 \pm 0.68$  μM were obtained. The goodness parameter was not



**Fig. 1.** Phlorizin binding to brush-border membrane vesicles in the presence of Na<sup>+</sup> or K<sup>+</sup>. The measurements were performed with brush-border membrane vesicles from outer cortex of pig kidneys which contained (a) 90 mM Na<sup>+</sup>, 50 mM K<sup>+</sup> and 20 μg valinomycin per ml or (b) 100 mM K<sup>+</sup>. (a) Phlorizin binding was measured after 10-min incubation of membrane vesicles with different phlorizin concentrations in the presence of 90 mM Na<sup>+</sup> and 50 mM K<sup>+</sup>. (b) Phlorizin binding was measured after 10-min incubation in the presence of 100 mM K<sup>+</sup>. The measurements were corrected for nonspecific binding as described under Materials and Methods. In the presented Scatchard plots mean values of three measurements with standard deviations are shown. The line in a was calculated by assuming the existence of two phlorizin binding sites. The line in b was calculated by assuming that in the presence of K<sup>+</sup> only one phlorizin binding site is detected in the measured concentration range

significantly different when the ratio between low and high affinity binding sites was fixed to one or not. However, the fit became worse when the ratio was fixed to 2 or 0.5 (*data not shown*). A worse fit was also obtained when one type of phlorizin binding site with negative cooperativity was assumed (*data not shown*). The binding measurements in the presence of K<sup>+</sup> could be fitted sufficiently with only one type of phlorizin binding site (Fig. 1b). For this binding site an apparent  $K_D$ -value of  $13.0 \pm 0.4$  μM was calculated. The total number of phlorizin binding sites ( $201 \pm 4$  pmol · (mg of protein)<sup>-1</sup>) was slightly smaller than that measured in the presence



**Fig. 2.** Competitive inhibition of phlorizin equilibrium binding at a high affinity phlorizin binding site measured in the presence of Na<sup>+</sup>. The measurements were performed as in Fig. 1a. Membrane vesicles from outer cortex were incubated for 10 min in the presence of 90 mM Na<sup>+</sup> and 10 mM K<sup>+</sup> with phlorizin concentrations between 0.05 and 1 μM. The incubation was performed either in the absence of phloretin (○) or in the presence of 25 (●), 100 (■) or 200 μM phloretin (▲). In the Scatchard plots mean values of three measurements with standard deviations are presented. The lines were calculated by linear regression analysis ( $r^2 > 93$ )

of 90 mM Na<sup>+</sup> plus 50 mM K<sup>+</sup>. The phlorizin binding measurements in the presence of 100 mM K<sup>+</sup> do not exclude the existence of two types of phlorizin binding sites. In fact a slightly better fit was obtained if a two-site model was employed (*data not shown*).

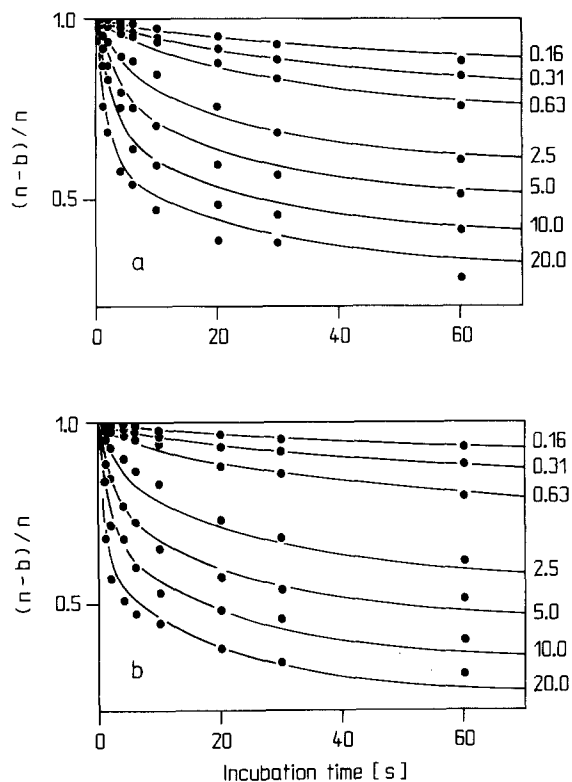
#### INHIBITION OF PHLORIZIN EQUILIBRIUM BINDING BY PHLORETIN

Since the phloretin moiety in the phlorizin molecule is required to observe high affinity binding to the Na<sup>+</sup>-D-glucose cotransporter it has been proposed that phlorizin may interact with two points at the D-glucose binding site [1, 6]. To test this hypothesis we measured whether phloretin, which is a non-competitive inhibitor of Na<sup>+</sup>-D-glucose cotransport [7], is able to competitively inhibit phlorizin binding to brush-border membrane vesicles from outer renal cortex. To investigate competition of phloretin at the presumed high affinity phlorizin binding site,

binding measurements with different phloretin concentrations were performed by incubating vesicles in the presence of 90 mM Na<sup>+</sup> plus 10 mM K<sup>+</sup> with phlorizin concentrations between 0.05 and 1 μM. Figure 2 shows that in the presence of Na<sup>+</sup> phlorizin binding to a high affinity site was competitively inhibited by phloretin. For the inhibition by phloretin a  $K_i$  value of  $98.4 \pm 4.8$  μM was calculated. By measuring the D-glucose inhibition of phlorizin binding in the same preparation, a competitive inhibition was observed also for D-glucose (*data not shown*). For the inhibition by D-glucose a  $K_i$  value of  $12.3 \pm 0.8$  mM was calculated. These data are consistent with the assumption that at a high affinity phlorizin binding site (in the presence of Na<sup>+</sup>) phlorizin interacts at two points with the Na<sup>+</sup>-D-glucose cotransporter: with the D-glucose moiety at a D-glucose binding site and with the phloretin moiety at a closely associated protein domain.

#### ONSET OF PHLORIZIN BINDING IN THE PRESENCE OF 90 mM Na<sup>+</sup>

To investigate the mechanism of phlorizin binding in the presence of 90 mM Na<sup>+</sup> on both membrane sides at zero membrane potential, membrane vesicles from outer cortex and outer medulla were prepared which contained 90 mM Na<sup>+</sup> plus 50 mM K<sup>+</sup> and 20 μg valinomycin per ml. The vesicles were incubated (30°C) with seven different phlorizin concentrations (0.16–20.0 μM) in a buffer containing 90 mM Na<sup>+</sup> plus 50 mM K<sup>+</sup>, and phlorizin equilibrium binding and the onset of phlorizin binding was measured. Curvilinear Scatchard plots similar to Fig. 1a were obtained for phlorizin equilibrium binding (incubation time 10 min). By fitting these binding curves to a two-site model  $252 \pm 5$  and  $250 \pm 15$  pmol · (mg of protein)<sup>-1</sup> total phlorizin binding sites were determined for outer cortex and outer medulla. To measure the time course of phlorizin binding after addition of seven phlorizin concentrations binding measurements were performed at eight different time intervals (Fig. 3). The various kinetic models were analyzed by solving the derived kinetic equations and by fitting them to the time courses of phlorizin association (*see Materials and Methods*). By a "one-site model" with two kinetic parameters the experimental data could not be fitted satisfactorily (Table 2). The fits could not be improved significantly by a "two-state, one-site model" (four parameters), in which an equilibrium between inactive and active phlorizin binding sites was assumed (Table 2). This suggests that recruitment of nonaccessible phlorizin binding sites did not significantly influence the binding measurements. This means that under the employed experi-



**Fig. 3.** Families of curves which were fitted to data, in which the onset of phlorizin binding to vesicles from outer cortex and outer medulla was measured in the presence of 90 mM Na<sup>+</sup> on both membrane sides. Membrane vesicles from (a) outer cortex and (b) outer medulla were prepared which contained 90 mM Na<sup>+</sup> plus 50 mM K<sup>+</sup> and 20 μg/ml of valinomycin. The vesicles were incubated with different concentrations of phlorizin in the presence of 90 mM Na<sup>+</sup> and 50 mM K<sup>+</sup> (30°C) and the onset of phlorizin binding was measured. In the graph the relative number of free phlorizin binding sites ( $n - b/n$ ) after different incubation times is plotted.  $b$  Represents the amount of bound phlorizin and  $n$  the total number of phlorizin binding sites which was determined by measuring phlorizin binding at equilibrium. The μM concentrations of phlorizin in the incubation media during the experiments are indicated on the right side of the curves. In the graph mean values of triplicate measurements are shown. The standard deviations are smaller than the symbol size. For clarity some phlorizin binding measurements obtained after 1 and 2 sec of incubation are not shown. The binding measurements were fitted according to the “two independent sites, two-step binding model.” In the fit the  $K_D$  of the low affinity site ( $k_3/k_4$ ) was fixed to a value of 7.9 μM which was determined from measurements of phlorizin equilibrium binding in membrane vesicles from outer cortex (see Fig. 1a). Furthermore  $k_6$  was fixed to a value of 1 which implies a 1 : 1 stoichiometry of high and low affinity phlorizin binding sites. The goodness of the fits were 0.0041 for outer cortex and 0.0033 for outer medulla. The constants for  $k_1$ ,  $k_2$  and  $k_3$  are given in Results

mental conditions (presence of Na<sup>+</sup> on both membrane sides, absence of D-glucose) most of the phlorizin binding sites are oriented outward. With a “two independent sites model” requiring five parameters significantly better fits were obtained (Ta-

**Table 2.** Evaluation of kinetic models for phlorizin binding to brush-border membrane vesicles from outer cortex and outer medulla<sup>a</sup>

Model	Goodness parameters	
	Outer cortex	Outer medulla
One site	0.0142	0.0096
Two states, one site	0.0142	0.0089
Two independent sites	0.0048	0.0033
Two dependent sites	0.0070	0.0040
One site, two-step binding	0.0070	0.0046
Two independent sites, two-step binding	0.0038	0.0029

<sup>a</sup> The onset of phlorizin binding in the presence of seven different phlorizin concentrations and 90 mM Na<sup>+</sup> plus 50 mM K<sup>+</sup> was measured at 30°C as described in Fig. 3. The vesicles contained 90 mM Na<sup>+</sup> plus 50 mM K<sup>+</sup> and were preincubated with 20 μg/ml of valinomycin. The relative numbers of free phlorizin binding sites after eight different times of incubation were calculated and the data were fitted with the six kinetic models described in Materials and Methods and Results. The goodness parameters of the fits were calculated from the weighted data (see Materials and Methods).

ble 2). In this model it is assumed that two phlorizin binding sites, which may be on the same or on different proteins, do not interconvert during the incubation with phlorizin. Testing whether the binding sites may interconvert, the “two dependent sites model” with five parameters was applied (Table 2). With this model very slow convergence was observed and the fit was inferior to that found with the “two independent sites model.” Since in the “two dependent sites model” the rate constants for the conversions of  $E_1$  to  $E_2$  and of  $E_2$  to  $E_1$  were rather small ( $<0.00004 \text{ sec}^{-1}$ ), this suggests that the two phlorizin binding sites do not convert after phlorizin has been added.

Since in the above reported inhibition experiments with D-glucose and phloretin, phlorizin interacts at two points with the Na<sup>+</sup>-D-glucose cotransporter, also a “one-site, two-step binding model” (four parameters) was tried. Table 2 shows that with this model fits were obtained which were significantly better than those found with the “one-site model” and the “two-states, one-site model.” For the vesicles from both kidney regions the first binding step was rapid whereas the second step was slow. Since for the first binding step the rate constant of association or that of dissociation could be fixed to high values without impairing the fit, this model is sufficiently described with three parameters. Finally, since the “one-site, two-step binding model” is consistent with the two-point-interaction hypothesis of phlorizin and since the onset of phlorizin binding in the presence of an inside-negative



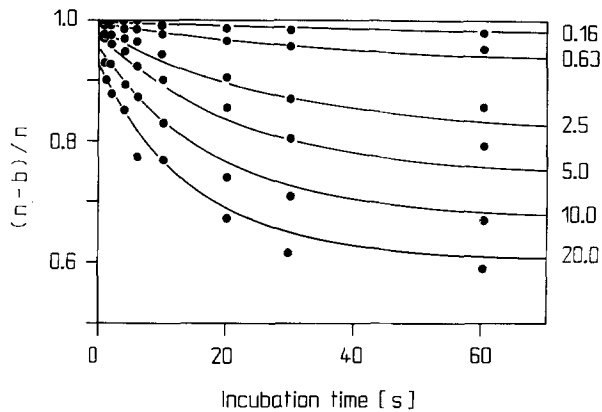
membrane potential could not be fitted by the "two independent sites model" when the rate constants of dissociation were fixed to values obtained with a clamped membrane potential (*see below*), both models were combined to the "two independent sites, two-step binding model." The reaction sequence of this model is presented in Materials and Methods (*see Eq. (6)*).

With this model the best fits were obtained for the phlorizin binding to membrane vesicles from outer cortex and outer medulla (*see Table 2*, goodness parameters: 0.0038 for outer cortex, 0.0029 for outer medulla). In outer cortex, the goodness parameter (0.0038) obtained for the "two independent sites, two-step binding model" was significantly better than the goodness parameter (0.0048) obtained for the "two independent sites model." When the data were fitted with the "two independent sites model" systematic deviations between experimental data and fitted curves became apparent. Good fits with the "two independent sites, two-step binding model" were also obtained for outer cortex (goodness parameter 0.0041) and outer medulla (goodness parameter 0.0033) if the dissociation constant for the low affinity phlorizin binding site ( $K_{D\text{low}} = k_5/k_4$ ) and the ratio between low and high affinity phlorizin binding sites ( $k_6$ ) were fixed to the respective values of 7.9  $\mu\text{M}$  and 1.23 which were determined from the equilibrium measurements in membrane vesicles from outer cortex (*see Fig. 1a*). Figure 3 shows that fits of identical quality were obtained for outer cortex and outer medulla if  $k_5/k_4$  and  $k_6$  were fixed to 7.9  $\mu\text{M}$  and 1, respectively (goodness parameters: 0.0041 for outer cortex, 0.0033 for outer medulla). When  $k_6$  was fixed to 0.66, 0.5 or 0.33 the fits became worse whereas fits of similar quality were obtained when  $k_6$  was fixed to 2 or 3. The  $K_D$  values of the high affinity binding site in outer cortex and outer medulla calculated after fixing of  $k_6$  to 0.66, 0.5 or 0.33 were significantly higher, and the  $K_D$  values calculated after fixing of  $k_6$  to 2 or 3 were significantly lower than those obtained from equilibrium binding measurements (*data not shown*). Only after fixing of  $k_6$  to 1, for the low and the high affinity phlorizin binding sites in outer cortex and outer medulla  $K_D$  values were calculated which did not differ significantly from those obtained from equilibrium binding measurements (for outer cortex, *see below* and Fig. 1a; for outer medulla, *data not shown*). Thus, our data suggest a 1 : 1 stoichiometry of low and high affinity phlorizin binding sites in outer cortex and outer medulla. After fixing of  $k_5/k_4$  to 7.9  $\mu\text{M}$  and of  $k_6$  to 1, for  $k_1$ ,  $k_2$  and  $k_3$  the following constants were determined for outer cortex and outer medulla (with standard deviations expressed as percentages):  $k_1$  ( $\mu\text{M}^{-1}$ ) 1.52 (27%), 0.40 (14%);  $k_2$  ( $\text{sec}^{-1}$ ) 0.027

(7%), 0.048 (5%);  $k_3$  ( $\text{sec}^{-1}$ ) 0.013 (34%), 0.013 (27%). The dissociation constants of the high affinity phlorizin binding site in outer cortex and outer medulla which can be calculated from these constants ( $k_{D\text{high}} = k_3 \cdot k_1^{-1} \cdot k_2^{-1}$ ) are  $0.32 \pm 0.14$  and  $0.66 \pm 0.20 \mu\text{M}$ , respectively.

#### ONSET OF PHLORIZIN BINDING IN THE PRESENCE OF 3 mM Na<sup>+</sup>

The effect of Na<sup>+</sup> was investigated by measuring the onset of phlorizin binding to brush-border membrane vesicles from renal outer cortex in the presence of 97 mM K<sup>+</sup>, 20  $\mu\text{g}/\text{ml}$  of valinomycin and 3 mM Na<sup>+</sup> on both membrane sides. The measurements were performed at 30°C with six different phlorizin concentrations (0.16–20  $\mu\text{M}$ ). The total number of phlorizin binding sites, which was measured after 10 min incubation and calculated by fitting the curvilinear Scatchard plot with a two-sites model, was  $250 \pm 18 \text{ pmol} \cdot (\text{mg of protein})^{-1}$ . Trying to fit the data to different models, the respective goodness parameters were obtained: "one-site model" 0.0050; "two-states, one-site model" 0.0050; "two independent sites model" 0.0028; "two dependent sites model" 0.0032; "one-site, two-step binding model" 0.0036; "two independent sites, two-step binding model" 0.0023. Again the best fit was obtained with the "two independent sites, two-step binding model." Furthermore, with the "two independent sites, two-step binding model" an optimal fit (goodness parameter of 0.0023) was also obtained if a 1 : 1 stoichiometry of low and high affinity binding sites was assumed by fixing  $k_6$  to 1 (Fig. 4). Since fixing of  $k_6$  to 1 gave optimal fits with all experiments described in this paper (*see below*) and since only after fixing of  $k_6$  to 1 the same  $K_D$  values were obtained from onset curves of phlorizin binding measured in the presence of 90 mM Na<sup>+</sup> and from equilibrium binding measurements in the presence of 90 mM Na<sup>+</sup> (*see above*), low and high affinity phlorizin binding sites in brush-border membranes are supposed to be present at a ratio of 1 : 1. Therefore, in the following, constants will be reported which were obtained when  $k_6$  was fixed to 1. From the the binding measurements performed in the presence of 3 mM Na<sup>+</sup> on both membrane sides (Fig. 4) the following constants were calculated:  $k_1 = 0.107 \pm 0.009 \mu\text{M}^{-1}$ ,  $k_2 = 0.062 \pm 0.003 \text{ sec}^{-1}$ ,  $k_3 = 0.024 \pm 0.004 \text{ sec}^{-1}$ ,  $k_5/k_4 = 112.1 \pm 28.0 \mu\text{M}$ . The dissociation constants for the low and high affinity phlorizin binding sites were  $112.1 \pm 28.0 \mu\text{M}$  ( $k_5/k_4$ ) and  $3.63 \pm 0.70 \mu\text{M}$  ( $k_3 \cdot k_1^{-1} \cdot k_2^{-1}$ ), respectively. Thus the affinities of both the low and the high affinity phlorizin binding sites are increased after binding of Na<sup>+</sup>. To identify

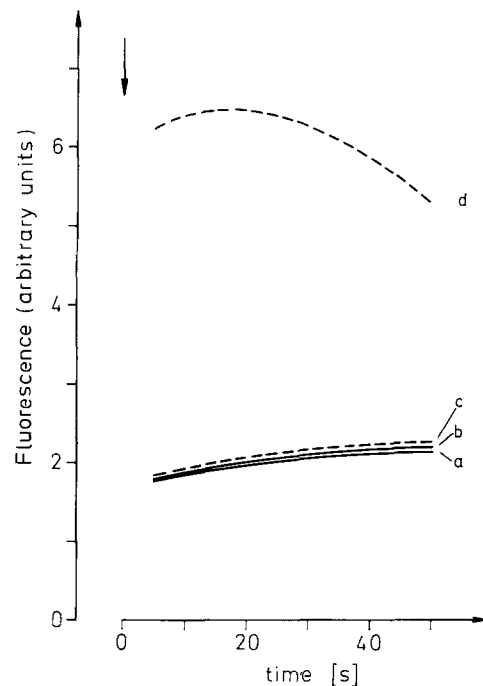


**Fig. 4.** Family of curves fitted to data, in which the onset of phlorizin binding to membrane vesicles from outer cortex was measured in the presence of 3 mM Na<sup>+</sup> on both membrane sides. Membrane vesicles from outer cortex were prepared which contained 97 mM K<sup>+</sup> plus 3 mM Na<sup>+</sup> and were incubated with 20 μg/ml of valinomycin. The vesicles were incubated with different concentrations of phlorizin in the presence 97 mM K<sup>+</sup> plus 3 mM Na<sup>+</sup> (30°C). The measurements were performed and the data are presented as in Fig. 3. The curves were fitted according to the "two independent sites, two-step binding model." In the fit  $k_6$  was fixed to 1. The goodness of the fit was 0.0023. The constants calculated for  $k_1$ ,  $k_2$ ,  $k_3$  and  $k_5/k_4$  are given in Results

the constants of the "two independent sites, two-step binding model" which are changed by Na<sup>+</sup> binding to the transporters the data measured in the presence of 3 mM Na<sup>+</sup> were fitted when  $k_6$  was fixed to 1 and the other constants were fixed to the values which had been obtained in the presence of 90 mM Na<sup>+</sup> (see Fig. 3a). When in addition to  $k_6$  different constants were fixed the following goodness parameters were calculated: no additional constant fixed, 0.0023;  $k_1$  fixed, 0.0050;  $k_2$  fixed, 0.0027;  $k_3$  fixed, 0.0025;  $k_5/k_4$  fixed, 0.0244. The data demonstrate that the affinity of both phlorizin binding sites is increased by Na<sup>+</sup>. They suggest that Na<sup>+</sup> increases the affinity of phlorizin binding to the high affinity binding site by increasing the first binding step ( $k_1$ ).

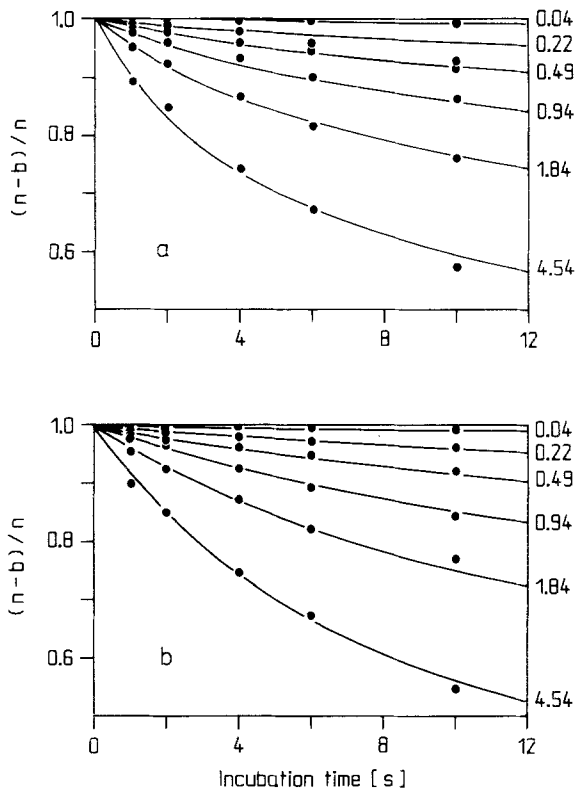
#### ONSET OF PHLORIZIN BINDING TO MEMBRANE VESICLES MEASURED IN THE PRESENCE OF Na<sup>+</sup>-GRADIENTS

To investigate whether Na<sup>+</sup> binding to the outside or to the inside of membrane vesicles has an effect on phlorizin binding the onset of phlorizin binding was also investigated when initially either 90 or 3 mM Na<sup>+</sup> was only present on the outside of the vesicles. In the first set of experiments membrane vesicles from outer cortex and outer medulla were preloaded with 100 mM potassium cyclamate and



**Fig. 5.** Estimation of the membrane potential of K<sup>+</sup>-containing brush-border membrane vesicles with and without valinomycin which were incubated in buffers containing K<sup>+</sup> or Na<sup>+</sup>. Brush-border membrane vesicles from outer cortex, at a protein concentration of 5 mg/ml, were preloaded with 100 mM K<sup>+</sup> (KC buffer) and incubated for 10 min (30°C) in the absence (experiments *a* and *b*, solid lines) and presence of 20 μg per ml of valinomycin (experiments *c* and *d*, broken lines). At time 0 (see arrow) 20 μl of the membrane vesicles was added to a stirred cuvette which was filled with 2 ml of buffers (28–30°C) to which 3 μM of diethylthiadiazinecarbocyanine iodide had been added. The buffers contained 20 mM imidazole cyclamate, pH 7.4, 0.1 mM magnesium cyclamate plus either 100 mM potassium cyclamate (*a* and *c*) or plus 10 mM potassium cyclamate and 90 mM sodium cyclamate (*b* and *d*). Excitation was at 622 nm and emission at 670 nm. A representative example of three independent experiments is presented

incubated (30°C) in buffers containing 90 mM sodium cyclamate, 10 mM potassium cyclamate and different phlorizin concentrations (0.04, 0.22, 0.49, 0.94, 1.94 and 4.54 μM). Phlorizin binding was measured at five different time intervals (1 to 10 sec) after the addition of phlorizin (see Fig. 6). Employing the cyanine dye diethylthiadiazinecarbocyanine iodide it was found that no significant membrane potential was generated by the Na<sup>+</sup> gradient (Fig. 5). Control experiments, in which <sup>22</sup>Na<sup>+</sup> was employed to measure the intravesicular Na<sup>+</sup> concentration, revealed that the Na<sup>+</sup> concentration in the vesicles was 10.0 ± 1.1 mM after 10-sec incubation of the vesicles with 90 mM Na<sup>+</sup> (data not shown). The total numbers of phlorizin binding sites in these ex-

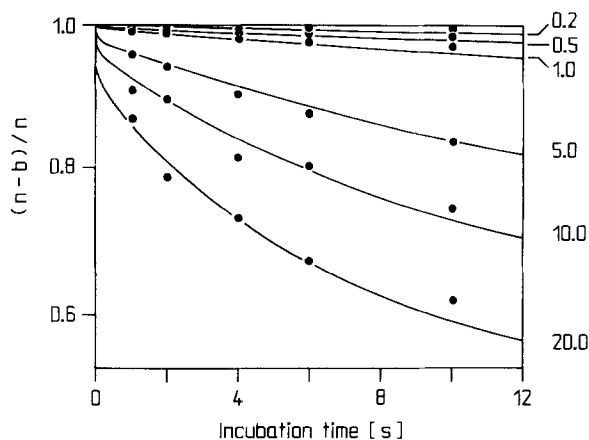


**Fig. 6.** Family of curves fitted to data, in which the onset of phlorizin binding to membrane vesicles from outer cortex and outer medulla was measured in the presence of an inwardly directed initial gradient of 90 mM Na<sup>+</sup>. Membrane vesicles from (a) outer renal cortex and (b) outer medulla containing 100 mM K<sup>+</sup> were incubated (30°C) with different concentrations of phlorizin in the presence of 90 mM Na<sup>+</sup> plus 10 mM K<sup>+</sup>. The measurements were performed and the data are presented as in Fig. 3. The data were fitted according to the “two independent sites, two-step binding model” and a 1 : 1 stoichiometry of low and high affinity phlorizin binding sites was assumed ( $k_6$  was fixed to 1).  $k_5/k_4$  was fixed to 7.9  $\mu\text{M}$  and  $k_3$  to 0.013  $\text{sec}^{-1}$ . These values were obtained from measurements in which 90 mM Na<sup>+</sup> was present on both membrane sides (see Fig. 1a, Fig. 3). The goodness of the fit was 0.0080 for outer cortex and 0.0038 for outer medulla. The constants calculated for  $k_1$  and  $k_2$  are given in Results

periments which were determined from equilibrium binding measurements were  $222 \pm 9 \text{ pmol} \cdot (\text{mg of protein})^{-1}$  in outer cortex and  $223 \pm 7 \text{ pmol} \cdot (\text{mg of protein})^{-1}$  in outer medulla. Since these experiments were performed over a short time period and the Na<sup>+</sup> concentration in the vesicles changed during the course of the experiments, the measurements were not used to distinguish between the different phlorizin binding models but fitted to the “two independent sites, two-step binding model” and the constants obtained in this model were compared with those obtained in the presence of Na<sup>+</sup> equilibrium. The goodness parameters of the fits ob-

tained with the “two independent sites, two-step binding model” were 0.0079 for outer cortex and 0.0040 for outer medulla. Identical goodness parameters were obtained if a 1 : 1 stoichiometry of high and low affinity phlorizin binding sites was assumed ( $k_6$  was fixed to 1). Figure 6 shows fits in which  $k_6$  was fixed to 1 and  $k_5/k_4$  (dissociation constant of the low affinity phlorizin binding site) plus  $k_3$  were fixed to the values which were obtained at equilibrium of 90 mM Na<sup>+</sup> (see Fig. 3,  $k_5/k_4 = 7.9 \mu\text{M}$ ,  $k_3 = 0.013 \text{ sec}^{-1}$ ). Under these conditions about the same goodness parameters (outer cortex 0.0080; outer medulla 0.0038) were obtained as without fixing of constants (see above). The values which were calculated for  $k_1$  (outer cortex,  $k_1 = 0.20 \pm 0.01 \mu\text{M}^{-1}$ ; outer medulla,  $k_1 = 0.13 \pm 0.01 \mu\text{M}^{-1}$ ) were lower and the values which were calculated for  $k_2$  (outer cortex  $k_2 = 0.13 \pm 0.01 \text{ sec}^{-1}$ , outer medulla  $k_2 = 0.23 \pm 0.01 \text{ sec}^{-1}$ ) were higher as those calculated from the measurements performed at Na<sup>+</sup> equilibrium. For the dissociation constants of the high affinity phlorizin binding sites in outer cortex and outer medulla ( $K_{D\text{high}} = k_3 \cdot k_1^{-1} \cdot k_2^{-1}$ ) about the same values were obtained (outer cortex,  $0.48 \pm 0.17 \mu\text{M}$ ; outer medulla,  $0.44 \pm 0.12 \mu\text{M}$ ) as in the presence of Na<sup>+</sup> equilibrium (see above, outer cortex  $0.32 \pm 0.14 \mu\text{M}$ ; outer medulla  $0.66 \pm 0.20 \mu\text{M}$ ).

In a second set of experiments, phlorizin binding in the presence of an initial Na<sup>+</sup> concentration difference of 3 mM (out > in) was compared with that in the presence of 3 mM Na<sup>+</sup> inside and outside the vesicles (compare experiments in Figs. 4 and 7). Membrane vesicles from outer cortex containing 100 mM K<sup>+</sup> were incubated (30°C) with 3 mM Na<sup>+</sup>, 97 mM K<sup>+</sup> and different phlorizin concentrations (0.2–20  $\mu\text{M}$ ). The total number of phlorizin binding sites, which was determined from Scatchard plots obtained after 10-min incubation (30°C) with phlorizin, was  $250 \pm 12 \text{ pmol} \cdot (\text{mg of protein})^{-1}$ . The onset of phlorizin binding was measured after five time intervals (1 to 10 sec) after the incubation with phlorizin. With the “two independent sites, two-step binding model” a good fit of the data was obtained which was not changed if a 1 : 1 stoichiometry of high and low affinity phlorizin binding sites was assumed by fixing  $k_6$  to 1 (goodness parameter 0.0022). Figure 7 shows that a good fit was also obtained (goodness parameter 0.0025) when  $k_6$ ,  $k_5/k_4$  and  $k_3$  were fixed to the values which were obtained for phlorizin binding in the presence of 3 mM Na<sup>+</sup> on both membrane sides (see Fig. 4,  $k_6 = 1$ ,  $k_5/k_4 = 112.1 \mu\text{M}$ ,  $k_3 = 0.024 \text{ sec}^{-1}$ ). Under these conditions a value of  $0.010 \pm 0.004 \mu\text{M}^{-1}$  was calculated for  $k_1$  and a value of  $0.76 \pm 0.03 \text{ sec}^{-1}$  for  $k_2$ . As was observed with 90 mM Na<sup>+</sup>,  $k_1$  was significantly lower and  $k_2$  was significantly higher as in the



**Fig. 7.** Family of curves fitted to data, in which the onset of phlorizin binding to membrane vesicles from outer cortex was measured in the presence of inwardly directed initial gradient of 3 mM Na<sup>+</sup>. Membrane vesicles from outer renal cortex containing 100 mM K<sup>+</sup> were incubated (30°C) with different phlorizin concentrations in the presence of 97 mM K<sup>+</sup> and 3 mM Na<sup>+</sup>. The measurements were performed and the data are presented as in Fig. 3. The data were fitted according to the "two independent sites, two-step binding model" and a 1:1 stoichiometry of low and high affinity phlorizin binding sites was assumed ( $k_6$  was fixed to 1).  $k_3/k_4$  and  $k_3$  were fixed to respective values of 112.1  $\mu\text{M}$  and 0.024  $\text{sec}^{-1}$  which were obtained for phlorizin binding in the presence of 3 mM Na<sup>+</sup> on both membrane sides (see Fig. 4). The goodness of the fit was 0.0025. The constants calculated for  $k_1$  and  $k_2$  are given in Results

presence of Na<sup>+</sup> equilibrium (compare with Fig. 4,  $k_1 = 0.107 \mu\text{M}^{-1}$ ,  $k_2 = 0.062 \text{sec}^{-1}$ ). For the dissociation constant of the high affinity phlorizin binding site ( $K_{D \text{ high}} = k_3 \cdot k_1^{-1} \cdot k_2^{-1}$ ) a value of  $3.13 \pm 1.36 \mu\text{M}$  was calculated which was not significantly different from the value of  $3.63 \pm 0.70 \mu\text{M}$  which was obtained at equilibrium of 3 mM Na<sup>+</sup>.

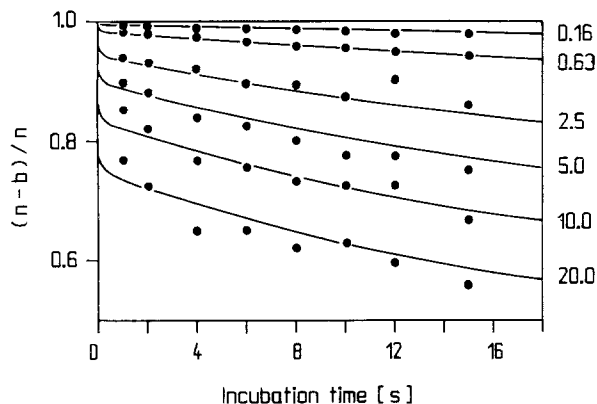
The data suggest that the observed Na<sup>+</sup>-induced affinity increase at the low and at the high affinity phlorizin binding site (compare Figs. 3 and 6 with Figs. 4 and 7) is due to Na<sup>+</sup> binding to the extracellular side of the brush-border membrane which corresponds to the outside of the membrane vesicles [11]. Although Na<sup>+</sup> binding to the intracellular side of the brush-border membrane does apparently not alter the  $K_{D \text{ high}}$  significantly, it may have an effect on the two-step binding mechanism at the high affinity phlorizin binding site.

#### EFFECT OF THE MEMBRANE POTENTIAL ON PHLORIZIN BINDING

It has been reported previously that by an inside-negative membrane potential, the rate constant for phlorizin association to membrane vesicles from

kidney and intestine is increased, whereas the rate constant of dissociation is not altered [2, 32, 33]. Thus, to further test the validity of the "two independent sites, two-step binding model" the association of phlorizin to membrane vesicles was compared in the absence and presence of an inside-negative membrane potential. First we investigated the potential effect on phlorizin binding measured in the presence of 3 mM Na<sup>+</sup> on both membrane sides, and then the potential effect on phlorizin binding measured in the presence of an initial Na<sup>+</sup> concentration difference of 90 mM Na<sup>+</sup> (out > in).

Membrane vesicles from outer cortex containing 97 mM K<sup>+</sup> plus 3 mM Na<sup>+</sup> and 20  $\mu\text{g}/\text{ml}$  of valinomycin were incubated at 30°C with 97 mM choline<sup>+</sup>, 3 mM Na<sup>+</sup>, 20  $\mu\text{g}/\text{ml}$  of valinomycin plus six different concentrations of phlorizin (0.16–20  $\mu\text{M}$ ) and phlorizin binding was measured after eight different time intervals (1 to 15 sec). From phlorizin equilibrium binding measurements the total number of phlorizin binding sites was determined to be  $242 \pm 15 \text{ pmol} \cdot (\text{mg of protein})^{-1}$ . For the different phlorizin binding models the following goodness parameters were obtained: "one-site model" 0.0080; "two-states, one-site model" 0.0076; "two independent sites model" 0.0038; "two dependent sites model" 0.0030; "one-site, two-step binding model" 0.0053; "two independent sites, two-step binding model" 0.0028. Note that also these data could not be fitted by models with one binding site including the "two-states, one-site model" which is able to describe a recruitment of inaccessible phlorizin binding sites. The best fit was obtained with the "two independent sites, two-step binding model." The goodness of the fit with this model (0.0028) remained identical if a 1:1 stoichiometry of high and low affinity phlorizin binding sites was assumed ( $k_6$  fixed to 1). We next tested whether the binding models are in agreement with the observation that the dissociation of bound phlorizin is not affected by the membrane potential [2, 33, H. Koepsell, unpublished observation in brush-border membrane vesicles from porcine renal cortex]. Thus, the phlorizin binding curves measured in the presence of a K<sup>+</sup> diffusion potential were fitted to different models when the rate constants for dissociation (see reaction schemes in Materials and Methods) were fixed to values which were obtained in the absence of a membrane potential. In the following the goodness parameters which were obtained without and with fixation of rate constants are presented: "one-site model," 0.0080 ( $k_2$  fixed: 0.0146); "two-states, one-site model," 0.0076 ( $k_4$  fixed: 0.0076); "two independent sites model," 0.0038 ( $k_2$  and  $k_4$  fixed: 0.0078); "two dependent sites model," 0.0030 ( $k_4$  fixed: 0.0119); "one-site, two-step binding model,"



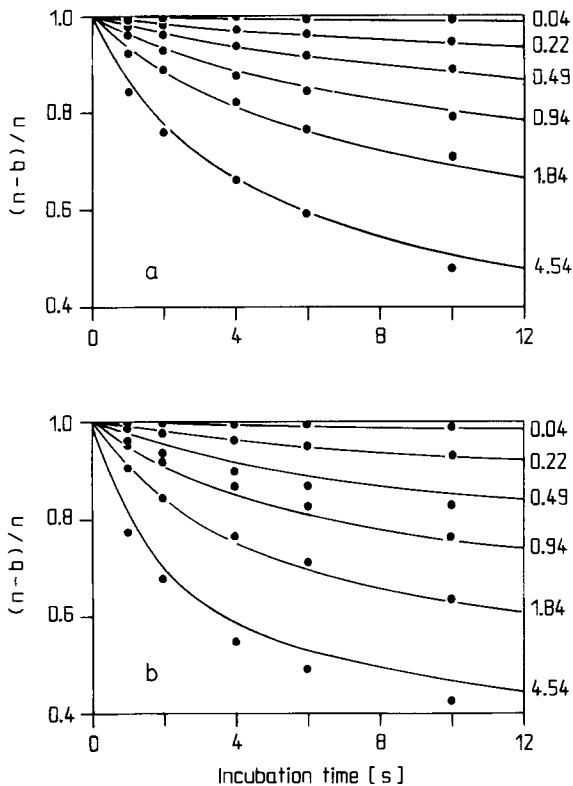
**Fig. 8.** Family of curves fitted to data, in which the onset of phlorizin binding to membrane vesicles from outer cortex was measured in the presence of 3 mM Na<sup>+</sup> on both membrane sides and of an inside-negative membrane potential. Membrane vesicles from outer renal cortex which contained 97 mM K<sup>+</sup> plus 3 mM Na<sup>+</sup> and were preincubated with 20 μg/ml of valinomycin were incubated (30°C) with different phlorizin concentrations in the presence of 97 mM choline<sup>+</sup> plus 3 mM Na<sup>+</sup>. The measurements were performed and the data are presented as in Fig. 3. The data were fitted according to the “two independent sites, two-step binding model” and a 1:1 stoichiometry of low and high affinity phlorizin binding sites was assumed ( $k_6$  was fixed to 1). The rate constants of dissociation  $k_3$  and  $k_5$  were fixed to respective values of 0.024 sec<sup>-1</sup> and 2349 sec<sup>-1</sup> · μM<sup>-1</sup> which were obtained in the absence of the valinomycin-induced membrane potential (see Fig. 4). The goodness of the fit was 0.0031. The constants calculated for  $k_1$ ,  $k_2$  and  $k_5/k_4$  are given in Results

0.0053 ( $k_2$  and  $k_4$  fixed: 0.0080); “two independent sites, two-step binding model,” 0.0028 ( $k_3$  and  $k_5$  fixed: 0.0028). Only with the “two-states, one-site model” and with the “two independent sites, two-step binding model” the quality of the fit was not reduced. Since with the “two-states, one-site model” the quality of the fit was significantly lower than with the “two independent sites, two-step binding model” the data are best described with the “two independent sites, two-step binding model.” Figure 8 shows a fit with this model when (i) the rate constants of dissociation  $k_3$  and  $k_5$  were fixed to the values of 0.024 sec<sup>-1</sup> and 2349 sec<sup>-1</sup> · μM<sup>-1</sup> which were obtained in the absence of the membrane potential (see Fig. 4) and (ii) a 1:1 stoichiometry of low and high affinity phlorizin binding sites was assumed ( $k_6$  was fixed to 1). The fit was nearly as good (goodness parameter 0.0031) as without fixation of any constant. For  $k_1$ ,  $k_2$  and  $k_5/k_4$  the following values were calculated:  $k_1 = 0.35 \pm 0.05 \mu\text{M}^{-1}$ ;  $k_2 = 0.037 \pm 0.002 \text{ sec}^{-1}$ ;  $k_5/k_4 = 20.6 \pm 1.8 \mu\text{M}$ . Thus in the presence of 3 mM Na<sup>+</sup> the dissociation constants of the high affinity phlorizin binding site ( $k_{D\text{high}} = k_3 \cdot k_1^{-1} \cdot k_2^{-1}$ ) and of the low affinity phlorizin binding site ( $k_{D\text{low}} = k_5 \cdot k_4^{-1}$ ) were  $1.87 \pm 0.42$

μM and  $20.6 \pm 1.8 \mu\text{M}$  in the presence of an inside-negative membrane potential, whereas the dissociation constants of the high and low affinity binding sites were  $3.63 \pm 0.70 \mu\text{M}$  and  $112.1 \pm 28.0 \mu\text{M}$  in the absence of a membrane potential (see Fig. 4). The experiments suggest that the affinity of low and high affinity phlorizin binding sites is increased by an inside-negative membrane potential.

In an attempt to investigate the effect of the membrane potential on phlorizin binding under conditions in which Na<sup>+</sup> gradient-dependent D-glucose uptake is measured, phlorizin binding measured in the presence of an initial concentration difference of 90 mM Na<sup>+</sup> (out > in) plus a valinomycin-induced diffusion potential of K<sup>+</sup> (Fig. 9) was compared with phlorizin binding measured in the absence of valinomycin (Fig. 6). Figure 5 shows that a vesicle inside-negative membrane potential was generated when the vesicles from outer cortex containing 100 mM potassium cyclamate were incubated with 90 mM sodium cyclamate plus 10 mM potassium cyclamate and valinomycin was present, whereas the membrane potential did not change when valinomycin was absent. Measurements of valinomycin induced uptake of (<sup>3</sup>H)tetraphenylphosphonium bromide into membrane vesicles from outer cortex and outer medulla showed that the valinomycin-induced inside-negative K<sup>+</sup> diffusion potential was identical in membrane vesicles from both kidney regions (data not shown). Figure 5 shows that during the first 10 sec of incubation with Na<sup>+</sup>-containing buffer the height of membrane potential which was generated in the presence of valinomycin changed only about 10% (Fig. 5). In the presence of valinomycin the Na<sup>+</sup> influx into the vesicles from outer cortex and outer medulla was slightly more rapid than in the absence of valinomycin. Thus after 10-sec incubation of the vesicles with 90 mM Na<sup>+</sup>, the Na<sup>+</sup> concentration in the vesicles from outer cortex and outer medulla was  $16.5 \pm 2.5$  and  $17.6 \pm 2.2$  mM, respectively. For the total numbers of phlorizin binding sites estimated from equilibrium binding measurements similar values as in the absence of valinomycin (see above, Fig. 6) were obtained: outer cortex  $223 \pm 7 \text{ pmol} \cdot (\text{mg of protein})^{-1}$ , outer medulla  $229 \pm 7 \text{ pmol} \cdot (\text{mg of protein})^{-1}$ .

The phlorizin binding measurements in outer cortex and outer medulla performed in the presence of valinomycin within 10 sec after incubation of the vesicles with Na<sup>+</sup> plus different phlorizin concentrations could be fitted with the “two independent sites, two step-binding model” (goodness parameters: outer cortex 0.059; outer medulla 0.0103). Figure 9 shows that about the same goodness parameters were obtained (outer cortex 0.0060, outer medulla 0.0106) if a 1:1 stoichiometry of the low



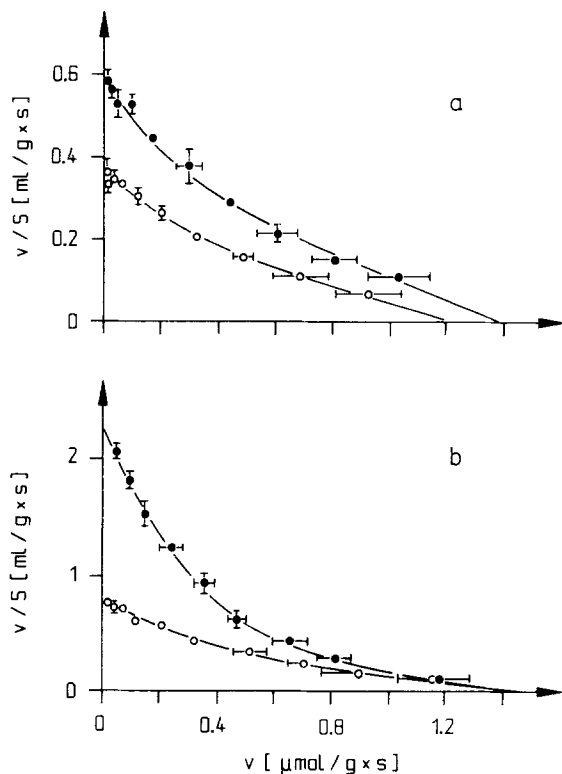
**Fig. 9.** Families of curves fitted to data, in which the onset of phlorizin binding to membrane vesicles from outer cortex and outer medulla was measured in the presence of an inwardly directed Na<sup>+</sup>-gradient plus a valinomycin-induced inside-negative membrane K<sup>+</sup>-diffusion potential. Membrane vesicles from (a) renal outer cortex and (b) outer medulla, which contained 100 mM K<sup>+</sup> and were preincubated with 20 μg/ml of valinomycin, were incubated (30°C) with different phlorizin concentrations in the presence of 90 mM Na<sup>+</sup> plus 10 mM K<sup>+</sup>. The measurements were performed and the data are presented as in Fig. 3. The data were fitted to the "two independent sites, two-step binding model" and a 1:1 stoichiometry of low and high affinity phlorizin binding sites was assumed ( $k_6$  was fixed to 1). The rate constants of dissociation  $k_3$  and  $k_5$  were fixed to the values which were obtained in the absence of the valinomycin-induced membrane potential (see Fig. 6, outer cortex:  $k_3 = 0.013 \text{ sec}^{-1}$ ,  $k_5 = 0.29 \text{ sec}^{-1}$ ; outer medulla:  $k_3 = 0.013 \text{ sec}^{-1}$ ,  $k_5 = 0.16 \text{ sec}^{-1}$ ). The goodness parameters were 0.0060 for outer cortex and 0.0103 for outer medulla. The  $K_D$  values calculated for the high and low affinity phlorizin binding site are given in Results

and high affinity phlorizin binding sites was assumed ( $k_6$  was fixed to 1) and the rate constants of phlorizin dissociation were fixed to the same values which were obtained in the absence of valinomycin (see Fig. 6, outer cortex:  $k_3 = 0.013 \text{ sec}^{-1}$ ,  $k_5 = 0.29 \text{ sec}^{-1}$ ; outer medulla:  $k_3 = 0.013 \text{ sec}^{-1}$ ,  $k_5 = 0.16 \text{ sec}^{-1}$ ). For the dissociation constants of high and low affinity phlorizin binding sites ( $K_{D \text{ high}} = k_3 \cdot k_1^{-1} \cdot k_2^{-1}$ ,  $K_{D \text{ low}} = k_5/k_4$ ) values of  $0.31 \pm 0.14$  and  $5.6 \pm 0.6 \mu\text{M}$  were calculated for outer cortex and values

of  $0.52 \pm 0.15$  and  $1.6 \pm 0.3 \mu\text{M}$  for outer medulla. A comparison of these data with the dissociation constant obtained at equilibrium of 90 mM Na<sup>+</sup> (Fig. 3) or in the presence of an initial concentration difference of 90 mM Na<sup>+</sup> (out > in) in the absence of valinomycin (Fig. 6) reveals that the affinity of the low affinity phlorizin binding site in outer medulla and probably also in the outer cortex was increased by the inside-negative membrane potential whereas the high affinity phlorizin binding sites were apparently not affected by the membrane potential.

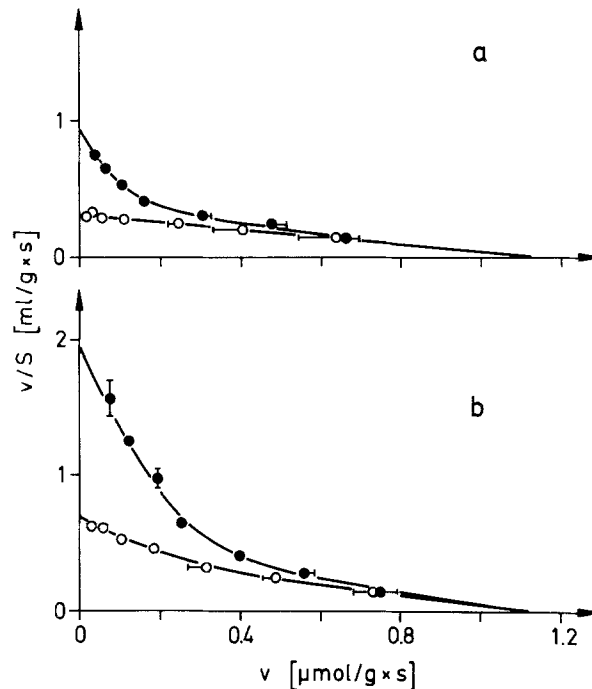
#### CHARACTERISTICS OF Na<sup>+</sup>-DEPENDENT D-GLUCOSE UPTAKE IN MEMBRANE VESICLES FROM OUTER CORTIX AND OUTER MEDULLA OF PORCINE KIDNEY

It was investigated whether the heterogeneity of Na<sup>+</sup>-dependent D-glucose transport described for outer cortex and outer medulla of rabbit kidneys [35–37] exists also in pig. Measuring the substrate dependence of Na<sup>+</sup> gradient-dependent D-glucose uptake in membrane vesicles from pig at 30°C (Fig. 10) and at 37°C (Fig. 11) in the absence and presence of valinomycin different kinetic properties were observed in outer cortex and outer medulla. Since the phlorizin binding data suggest that the Na<sup>+</sup>-D-glucose cotransporter in outer cortex and outer medulla is identical and contains two types of substrate binding sites, we tested whether the transport measurements in outer cortex and outer medulla could be fitted, when in outer cortex and outer medulla low and high affinity transport sites are assumed which have identical  $K_m$  values but different transport rates in outer cortex and outer medulla. Figures 10 and 11 show that this could be demonstrated in measurements which were performed under different experimental conditions. For D-glucose uptake in outer cortex and outer medulla measured at 30°C in the absence of valinomycin and in the presence of an initial concentration difference of 90 mM Na<sup>+</sup> (out > in) and 90 mM K<sup>+</sup> (in > out) apparent  $K_m$  values of  $0.37 \pm 0.09$  and  $3.94 \pm 0.21$  mM were obtained (Fig. 10). In the presence of valinomycin (30°C) for outer cortex apparent  $K_m$  values of  $0.37 \pm 0.04$  and  $3.94 \pm 0.15$  mM and for outer medulla apparent  $K_m$  values of  $0.2 \pm 0.01$  and  $3.94 \pm 0.20$  mM were calculated (Fig. 10). Thus, the membrane potential did not alter the apparent  $K_m$  values of low and high affinity transport in outer cortex but decreased the apparent  $K_m$  of high affinity transport in outer medulla. In outer cortex (30°C)  $V_{\text{max}(\text{total})}$  was slightly stimulated by valinomycin (absence of valinomycin:  $1193 \pm 26 \text{ pmol} \cdot$



**Fig. 10.** Substrate dependence of Na<sup>+</sup> gradient-dependent D-glucose uptake into membrane vesicles from outer cortex and outer medulla (30°C, absence and presence of inside-negative membrane potential), which was fitted by assuming two apparent transport sites in both kidney regions. Brush-border membrane vesicles from (a) outer cortex and (b) outer medulla of pig kidneys were loaded with 100 mM K<sup>+</sup> and preincubated without and with valinomycin. At 30°C initial L-glucose uptake rates were measured at K<sup>+</sup> equilibrium and initial D-glucose uptake rates were measured in the presence of initial concentration differences of 90 mM Na<sup>+</sup> (out > in) and 90 mM K<sup>+</sup> (in > out). The uptake rates which were stimulated by the Na<sup>+</sup> gradient over those measured at K<sup>+</sup> equilibrium were calculated. Open and filled symbols represent data obtained in the absence and presence of valinomycin, respectively. Mean values of three measurements with standard deviations are shown. The data which are presented according to Hofstee [13] were fitted as described in Materials and Methods. It was assumed that in each preparation two apparent transport sites are present. The fits were obtained when in both kidney regions a  $K_m$  value of 3.9 mM was assumed for the low affinity transport site (absence and presence of valinomycin). For the high affinity transport site a  $K_m$  value of 0.37 mM (outer cortex, absence and presence of valinomycin; outer medulla, absence of valinomycin) or a  $K_m$  value of 0.18 mM (outer medulla, presence of valinomycin) was obtained

mg<sup>-1</sup> · sec<sup>-1</sup>; presence of valinomycin: 1382 ± 44 pmol · mg<sup>-1</sup> · sec<sup>-1</sup>) whereas valinomycin did not significantly alter  $V_{max(total)}$  in outer medulla (absence of valinomycin: 1449 ± 33 pmol · mg<sup>-1</sup> · sec<sup>-1</sup>; presence of valinomycin: 1423 ± 47 pmol · mg<sup>-1</sup> · sec<sup>-1</sup>). In outer cortex  $V_{max}$  of high and low



**Fig. 11.** Substrate dependence of Na<sup>+</sup> gradient-dependent D-glucose uptake into membrane vesicles from outer cortex and outer medulla (37°C, absence and presence of inside-negative membrane potential), which was fitted by assuming two apparent transport sites with  $K_m$  values which are identical for both kidney regions. Brush-border membrane vesicles from (a) outer cortex and (b) outer medulla were loaded with 100 mM K<sup>+</sup>. At 37°C initial L-glucose uptake rates at K<sup>+</sup> equilibrium and initial D-glucose uptake rates in the presence of initial concentration differences of 90 mM Na<sup>+</sup> (out > in) and 90 mM K<sup>+</sup> (in > out) were measured in the absence or presence of valinomycin. Uptake rates of D-glucose stimulated by the Na<sup>+</sup> gradient over those of L-glucose measured at K<sup>+</sup> equilibrium were calculated and the data are presented as in Fig. 10. The data obtained in the absence of valinomycin (open symbols) and presence of valinomycin (filled symbols) were fitted separately. For the fit it was assumed that two apparent transport sites are present in outer cortex and outer medulla. In the absence of valinomycin in outer cortex only one  $K_m$  value of 3.7 mM could be detected (a, open symbols) whereas for the outer medulla one  $K_m$  value of 3.7 mM and another of 0.4 mM was estimated (b, open symbols). In the presence of valinomycin (filled symbols) for outer cortex and outer medulla a  $K_m$  value of 3.7 mM was obtained for the apparent low affinity transport site whereas for the apparent high affinity transport site a  $K_m$  value of 0.14 mM was calculated

affinity transport was stimulated by valinomycin (high affinity transport: from 44 ± 4 to 108 ± 7 pmol · mg<sup>-1</sup> · sec<sup>-1</sup>, low affinity transport: from 1149 ± 22 to 1275 ± 37 pmol · mg<sup>-1</sup> · sec<sup>-1</sup>). In outer medulla  $V_{max}$  of high affinity transport was stimulated whereas  $V_{max}$  of low affinity transport was de-

creased (high affinity transport: from  $159 \pm 5$  to  $361 \pm 5$  pmol · mg<sup>-1</sup> · sec<sup>-1</sup>; low affinity transport: from  $1291 \pm 27$  to  $1062 \pm 42$  pmol · mg<sup>-1</sup> · sec<sup>-1</sup>).

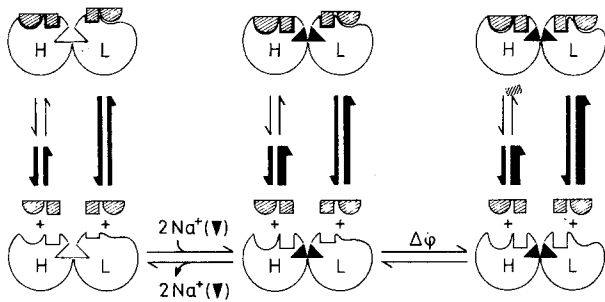
Na<sup>+</sup> gradient-dependent D-glucose uptake in outer cortex measured at 37°C in the absence of valinomycin could be fitted with one  $K_m$  value of  $3.69 \pm 0.10$  mM (Fig. 11a, open symbols). In contrast D-glucose uptake in the outer medulla measured in the absence of valinomycin at 37°C had to be fitted with two  $K_m$  values (Fig. 11b, open symbols). One value was the same as in outer cortex ( $3.69 \pm 0.11$  mM) and the other was about 10 times lower ( $0.40 \pm 0.02$  mM). Note that the  $K_m$  values obtained in the absence of valinomycin at 37°C were not significantly different from those estimated at 30°C (absence of valinomycin). The  $V_{max}$  values of D-glucose transport calculated at 37°C in the absence of valinomycin were  $1137 \pm 21$  pmol · mg<sup>-1</sup> · sec<sup>-1</sup> in outer cortex and  $1169 \pm 29$  pmol · mg<sup>-1</sup> · sec<sup>-1</sup> in outer medulla. Figure 11 shows that at 37°C the  $V_{max}$  values of D-glucose uptake in outer medulla and also in outer cortex were not increased by valinomycin. Thus, as was observed for outer medulla at 30°C, already in the absence of valinomycin the driving force of D-glucose uptake was maximal. After addition of valinomycin the  $K_m$  of the apparent low affinity transport site ( $3.7 \pm 0.3$  mM) remained unchanged in outer cortex and outer medulla. As was observed at 30°C in outer medulla also at 37°C the  $K_m$  value of high affinity transport in the outer medulla was increased by valinomycin (absence of valinomycin,  $0.40 \pm 0.02$  mM; presence of valinomycin  $0.14 \pm 0.01$  mM). Note that the apparent  $K_m$  value estimated at 37°C for the high affinity transport site in outer cortex and outer medulla (presence of valinomycin) was about the same as the  $K_m$  value estimated at 30°C for high affinity transport in outer medulla (presence of valinomycin,  $0.18 \pm 0.01$  mM). With the addition of valinomycin the  $V_{max}$  at the high affinity transport sites increased (outer cortex: from 0 to  $86 \pm 3$  pmol · mg<sup>-1</sup> · sec<sup>-1</sup>; outer medulla: from  $32 \pm 2$  to  $231 \pm 7$  pmol · mg<sup>-1</sup> · sec<sup>-1</sup>) whereas the  $V_{max}$  of the low affinity transport site decreased (outer cortex: from  $1137 \pm 20$  to  $1027 \pm 23$  pmol · mg<sup>-1</sup> · sec<sup>-1</sup>; outer medulla: from  $1003 \pm 24$  to  $928 \pm 42$  pmol · mg<sup>-1</sup> · sec<sup>-1</sup>).


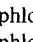
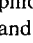
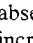
## Discussion

In membrane vesicles from renal proximal tubules the luminal side of the brush-border membranes is on the outer surface [11]. Phlorizin is a competitive inhibitor of Na<sup>+</sup>-D-glucose cotransport and interacts only with the outer surface of the vesicles. This

was shown in experiments where bound radioactive phlorizin could be removed within seconds (30°C, presence of 90 mM Na<sup>+</sup>) when an excess of nonradioactive phlorizin was added to the outside (H. Koepsell, *unpublished data*), and in experiments where Na<sup>+</sup> gradient-dependent D-glucose uptake could not be inhibited by 0.8 mM phlorizin when present inside the vesicles [19]. Phlorizin has a more than 100-fold higher affinity than D-glucose to the Na<sup>+</sup>-D-glucose cotransporter since its D-glucose moiety interacts with the D-glucose binding site and its phloretin moiety presumably with a hydrophobic protein domain near the D-glucose binding site. This notion is strongly supported by the finding that phlorizin binding is competitively inhibited by D-glucose and phloretin (Fig. 2). The exclusive high affinity phlorizin binding to the luminal side may be caused by an asymmetry of the transporter. During the transport cycle the D-glucose binding site may be accessible from both membrane surfaces whereas the phloretin binding domain of the transporter only from the luminal side. In the present study, families of onset curves of phlorizin binding to the outside of membrane vesicles from outer cortex and outer medulla could be fitted by a "two independent sites, two-step binding model" in which two types of Na<sup>+</sup>-dependent phlorizin binding sites were assumed which are present at a ratio of 1 : 1. It was shown that phlorizin binding to both sites was Na<sup>+</sup> dependent and that the association rate of phlorizin to both sites was dependent on the membrane potential. Our observation in pig that low and high affinity phlorizin binding sites are present at a ratio of 1 : 1 in outer cortex and in outer medulla is different to the observation of Turner and Moran in rabbit [37] who observed mainly high affinity phlorizin binding sites in outer cortex and high plus low affinity phlorizin binding sites in outer medulla. The different results in rabbit and pig may reflect species differences in phlorizin binding, however, they also may have been generated by the different experimental conditions which were employed for the phlorizin binding measurements. Turner and Moran [37] analyzed phlorizin binding in the presence of 60 mM Na<sup>+</sup> and subtracted non-specific phlorizin binding measured in the absence of Na<sup>+</sup>. In our investigation phlorizin binding was measured in the presence of 90 mM Na<sup>+</sup> and non-specific phlorizin binding was subtracted which was measured in the presence of 5 mM nonradioactive phlorizin (for details, *see* Materials and Methods). We have shown (*see* Fig. 1b) that phlorizin binding to the Na<sup>+</sup>-D-glucose cotransporter does not only occur in the presence of Na<sup>+</sup> but, with a more than 10-fold lower affinity, also in the absence of Na<sup>+</sup>. Thus, we do not believe that low affinity phlorizin





**Fig. 12.** Dimer model of Na<sup>+</sup>-D-glucose cotransporter in renal outer cortex and outer medulla. This model assumes that the functional Na<sup>+</sup>-D-glucose cotransporter contains a low affinity and a high affinity phlorizin binding site which are localized on two polypeptides (*H* and *L*) of the Na<sup>+</sup>-D-glucose cotransporter. It is further assumed that each polypeptide with a phlorizin binding site also contains a Na<sup>+</sup> binding site. Phlorizin is indicated by  where  represents the D-glucose moiety and  the phloretin moiety of phlorizin. Na<sup>+</sup> is represented by . Each phlorizin binding site contains a binding domain for D-glucose and phloretin. Phlorizin may bind to both binding sites in the absence and presence of Na<sup>+</sup>. Binding of Na<sup>+</sup> to the transporter increases the affinity of both phlorizin binding sites mainly by increasing the rate constants of phlorizin association (symbolized by the thickness of arrows). After saturation of the Na<sup>+</sup> binding sites (presence of 90 mM Na<sup>+</sup>) the phlorizin association to the low affinity site and the *K<sub>D</sub>* of this site may be furthermore increased by an inside-negative membrane potential.

binding sites of the Na<sup>+</sup>-D-glucose cotransporter can be determined correctly if phlorizin binding measured in the presence of Na<sup>+</sup> is corrected for the amount of phlorizin binding measured in the absence of Na<sup>+</sup>. Therefore it is very possible that the 1:1 ratio of low and high affinity phlorizin binding sites observed in porcine outer cortex and outer medulla may also be present in rabbit and other species. Notwithstanding that in porcine outer cortex and outer medulla the presence of separate Na<sup>+</sup>-D-glucose cotransporters with either low and or high affinity phlorizin binding sites which are present at a ratio of 1:1 cannot be excluded we would like to raise the hypothesis that the observed low and high affinity phlorizin binding sites do not belong to different transporter populations from different nephron regions but are localized on one functional Na<sup>+</sup>-D-glucose cotransporter molecule. This hypothesis is in agreement with data in which functional molecular weights of 230,000 and 110,000 have been determined for phlorizin binding by target size analysis [23, 31, 34] and polypeptides with the molecular weights of 75,000 and 47,000 have been identified as components of the renal Na<sup>+</sup>-D-glucose cotransporter which contain D-glucose binding sites [18, 26]. Thus, it may be assumed that both phlorizin binding sites are localized on two polypeptides which are components of one func-

tional Na<sup>+</sup>-D-glucose cotransporter. Whether these polypeptides are transporter subunits with the molecular weights of 75,000 and 47,000 or identical monomers with the molecular weights of either 75,000 or 47,000 is not known since it has not been clarified whether the *M<sub>r</sub>* 47,000 component of the Na<sup>+</sup>-D-glucose cotransporter is a transporter subunit or a proteolytic splitting product of the 75,000 polypeptide [for discussion, *see* 10, 20]. Figure 12 shows a model of the transporter in which two identical polypeptide monomers are assumed which contain a high affinity and a low affinity phlorizin binding site (*see L* and *H* in Fig. 12). In the model, phlorizin binding to both binding sites occurs in the absence and presence of Na<sup>+</sup>. To the high affinity site phlorizin binds in two steps. This binding is slow whereas phlorizin binding to the low affinity site is rapid. The experiments showed that sodium increased the affinity of both phlorizin binding sites (*see* Fig. 12). As has been described in membrane vesicles from rabbit kidney [2] we also observed in pig that the rate of phlorizin association to membrane vesicles was increased by Na<sup>+</sup>. Since this effect was observed independently whether Na<sup>+</sup> was added to both membrane sides or to the outside of right side-out oriented membrane vesicles (*compare* Figs. 4 and 3, and 7 and 6), Na<sup>+</sup> binding to the extracellular side of the transporter is apparently sufficient to increase the affinity of both phlorizin binding sites.

Earlier it had been reported that the rate of phlorizin association to brush-border membrane vesicles from rabbit kidney and intestine was increased by an inside-negative membrane potential [2, 32, 33] whereas the membrane potential did not alter the dissociation rate of bound phlorizin [2, 32]. We were able to confirm and extend these observations in measurements with brush-border membrane vesicles from pig kidney outer cortex and outer medulla (*see above*, H. K. Koepsell, *unpublished data*). Previously the effect of the membrane potential on phlorizin binding was explained as a potential effect on the recruitment of phlorizin binding sites on the extracellular side of the brush-border membrane and it was speculated that the unloaded transporter or a part thereof is negatively charged [30, 33]. Our results show that this interpretation is not sufficient to explain the experimental data if only one type of phlorizin binding sites is assumed. Thus, the phlorizin binding measurements could not be fitted with the "two-states, one-site binding" model, which assumes that one population of phlorizin binding sites can be present in an inactive and in an active form. Although by the "two independent sites, two-step binding model" the effects of membrane potential on phlorizin bind-

ing can be explained without assuming recruitment of phlorizin binding sites, potential-dependent recruitment of the low and/or the high affinity phlorizin binding sites cannot be excluded. Recently an alternative explanation was proposed [15]: Based on the observation that Na<sup>+</sup> binding to avian intestinal cells is potential dependent, it was suggested that the effect of the membrane potential on phlorizin association may be secondary to a potential-induced increase of Na<sup>+</sup> binding to one of two Na<sup>+</sup> binding sites. Furthermore it was speculated that phlorizin debinding may not be influenced by the membrane potential since it may require potential-independent debinding of Na<sup>+</sup> from a second Na<sup>+</sup> binding site [15]. Our data are in accordance with this hypothesis since we observed that the affinity of low and high affinity phlorizin binding sites was increased when Na<sup>+</sup> was added and when in the presence of low Na<sup>+</sup> concentrations an inside-negative membrane potential was applied.

Since the data on phlorizin binding described in this paper suggest that identical types of Na<sup>+</sup>-D-glucose cotransporters are present in porcine outer cortex and outer medulla which contain each a low affinity and a high affinity phlorizin binding site, one would like to know (i) whether the D-glucose domains of the low and the high affinity phlorizin binding sites are engaged in D-glucose cotransport and (ii) whether in outer cortex and outer medulla identical or different Na<sup>+</sup>-D-glucose cotransporter molecules exist. In agreement with measurements performed on membrane vesicles from outer cortex and outer medulla of rabbit kidneys [36], we also found in porcine kidney that the substrate dependence of Na<sup>+</sup> gradient-dependent D-glucose uptake was different in membrane vesicles from outer cortex and outer medulla (Figs. 10 and 11). In addition we observed that the substrate dependence in outer cortex and outer medulla was altered when temperature and the membrane potential were changed. Some investigators primarily observed low affinity Na<sup>+</sup>-D-glucose cotransport in the outer cortex and high affinity transport in the outer medulla and proposed the existence of a low affinity, high capacity transport system in outer cortex and of a high affinity, low capacity transport system in outer medulla. They determined a Na<sup>+</sup>/D-glucose stoichiometry of approximately 1 : 1 in outer cortex and of 2 : 1 in the outer medulla [35–37]. Performing transport measurements over a broad range of D-glucose concentrations, we detected both high plus low affinity transport in membrane vesicles from both outer cortex and outer medulla (see Figs. 10 and 11). A similar observation was recently made by Blank and coworkers [3] who measured low affinity, high capacity Na<sup>+</sup>-D-glucose cotransport plus high affinity,

low capacity Na<sup>+</sup>-D-glucose cotransport in membrane vesicles from outer renal cortex of rat.

From D-glucose uptake measurements one cannot distinguish between (i) transport sites on separate transporters, (ii) separate transport sites on one transporter, (iii) one transport site with changing affinity during the transport cycle or (iv) a transport site plus a regulatory Na<sup>+</sup>-dependent D-glucose binding site. Since we observed low and high affinity phlorizin binding sites with a stoichiometry of one in outer cortex and outer medulla, our working hypothesis was that one functional Na<sup>+</sup>-D-glucose cotransporter molecule has a low and a high affinity D-glucose transport site and we tried to fit Na<sup>+</sup> gradient-dependent D-glucose uptake by assuming two coexisting D-glucose transport sites. We observed that alterations of temperature or membrane potential had differential effects on the maximal velocity of high or low affinity Na<sup>+</sup>-D-glucose cotransport. These observations do not contradict the hypothesis that high and low affinity transport is catalyzed by one transporter since temperature or membrane potential may have differential effects on either two transport sites or two operational modes of one transporter. Our phlorizin binding data suggested that the Na<sup>+</sup>-D-glucose cotransporter is identical in outer cortex and outer medulla. We therefore tried to fit Na<sup>+</sup>-D-glucose cotransport in outer cortex and outer medulla by assuming identical  $K_m$  values for the respective low or high affinity transport sites. This was possible under nearly all experimental conditions. The only exception was that at 30°C an inside-negative membrane potential increased the affinity of high affinity transport in outer medulla but not in outer cortex. However, since in outer cortex the apparent  $K_m$  value of high affinity transport measured at 37°C in the presence of an inside-negative membrane potential was about the same as the values obtained for outer medulla at 30 and 37°C, identity of the high affinity transport in outer cortex and outer medulla can be assumed. The observed differences in the kinetics of Na<sup>+</sup>-D-glucose cotransport in outer cortex and outer medulla may reflect different lipid environments of the transporters [5] or different associated proteins in both kidney regions.

Our data are consistent with the hypotheses (i) that two populations of Na<sup>+</sup>-D-glucose cotransporters with low and high affinity phlorizin binding sites are present at a ratio of 1 : 1 in porcine outer cortex and outer medulla and (ii) that the Na<sup>+</sup>-D-glucose cotransporter in porcine outer cortex and outer medulla contains two D-glucose transport sites and is identical in both kidney regions. Since we observed that in the presence of 90 mM Na<sup>+</sup> by an inside-negative membrane potential the  $K_D$  of

low affinity phlorizin binding was decreased whereas the apparent  $K_m$  of high affinity Na<sup>+</sup>-glucose cotransport was decreased our data suggest that the low and high affinity phlorizin binding sites represent high and low affinity D-glucose transport sites, respectively.

This study was supported by the Deutsche Forschungsgemeinschaft (SFB 169).

## References

- Alvarado, F. 1967. Hypothesis for the interaction of phlorizin and phloretin with membrane carriers for sugars. *Biochim. Biophys. Acta* **135**:483–495
- Aronson, P.S. 1978. Energy-dependence of phlorizin binding to isolated renal microvillus membranes. *J. Membrane Biol.* **42**:81–98
- Blank, M.E., Bode, F., Baumann, K., Diedrich, D.F. 1989. Computer analysis reveals changes in the renal Na<sup>+</sup>/glucose cotransporter in diabetic rats. *Am. J. Physiol.* **257**:C385–C396
- Brot-Laroche, E., Serrano, M.-A., Delhomme, B., Alvarado, F. 1986. Temperature sensitivity and substrate specificity of two distinct Na<sup>+</sup>-activated D-glucose transport systems in guinea pig jejunal brush border membrane vesicles. *J. Biol. Chem.* **261**:6168–6176
- Corda, D., Pasternak, C., Shinitzky, M. 1982. Increase in lipid microviscosity of unilamellar vesicles upon the creation of transmembrane potential. *J. Membrane Biol.* **65**:235–242
- Diedrich, D.F. 1963. The comparative effects of some phlorizin analogs on the renal reabsorption of glucose. *Biochim. Biophys. Acta* **71**:688–700
- Diedrich, D.F. 1966. Competitive inhibition of intestinal glucose transport by phlorizin analogs. *Arch. Biochem. Biophys.* **117**:248–256
- Fritzsche, G.K. 1985. A kinetic analysis of enzyme inactivation as applied to the covalent modification of Na<sup>+</sup> + K<sup>+</sup>-ATPase and Ca<sup>2+</sup>-ATPase. *J. Theor. Biol.* **117**:397–415
- Fritzsche, G., Koepsell, H. 1983. An analysis of biphasic time courses: The inactivation of (Na<sup>+</sup> + K<sup>+</sup>)-ATPase and Ca<sup>2+</sup>-ATPase by ATP-analogs. *J. Theor. Biol.* **102**:469–476
- Haase, W., Koepsell, H. 1989. Electron microscopic immunohistochemical localization of components of Na<sup>+</sup>-cotransporters along the rat nephron. *Eur. J. Cell Biol.* **48**:360–374
- Haase, W., Schäfer, A., Murer, H., Kinne, R. 1978. Studies on the orientation of brush-border membrane vesicles. *Biochem. J.* **172**:57–62
- Hediger, M.A., Coady, M.J., Ikeda, T.S., Wright, E.M. 1987. Expression cloning and cDNA sequencing of the Na<sup>+</sup>/glucose co-transporter. *Nature (London)* **330**:379–381
- Hofstee, B.H.F. 1955. Graphical analysis of single enzyme systems. *Enzymologia* **17**:273–278
- Kessler, M., Semenza, G. 1983. The small-intestinal Na<sup>+</sup>, D-glucose cotransporter: An asymmetric gated channel (or pore) responsive to  $\Delta\psi$ . *J. Membrane Biol.* **76**:27–56
- Kimmich, G.A., Randles, J. 1988. Na<sup>+</sup>-coupled sugar transport: Membrane potential-dependent  $K_m$  and  $K_i$  for Na<sup>+</sup>. *Am. J. Physiol.* **255**:C486–C494
- Koepsell, H. 1986. Methodological aspects of purification and reconstitution of transport proteins from mammalian plasma membranes. *Rev. Physiol. Biochem. Pharmacol.* **104**:65–137
- Koepsell, H., Korn, K., Ferguson, D., Menuhr, H., Ollig, D., Haase, W. 1984. Reconstitution and partial purification of several Na<sup>+</sup> cotransport systems from renal brush-border membranes. Properties of the L-glutamate transporter in proteoliposomes. *J. Biol. Chem.* **259**:6548–6558
- Koepsell, H., Korn, K., Raszeja-Specht, A., Bernotat-Danielowski, S., Ollig, D. 1988. Monoclonal antibodies against the renal Na<sup>+</sup>-D-glucose cotransporter. Identification of antigenic polypeptides and demonstration of functional coupling of different Na<sup>+</sup>-cotransport systems. *J. Biol. Chem.* **263**:18419–18429
- Koepsell, H., Madrala, A. 1987. Interaction of phlorizin with the Na<sup>+</sup>-D-glucose cotransporter from intestine and kidney. *Topics Mol. Pharmacol.* **4**:169–202
- Koepsell, H., Menuhr, H., Ducis, I., Wissmüller, T.F. 1983. Partial purification and reconstitution of the Na<sup>+</sup>-D-glucose cotransport protein from pig renal proximal tubules. *J. Biol. Chem.* **258**:1888–1894
- Koepsell, H., Seibicke, S. 1990. Reconstitution and fractionation of renal brush-border transport proteins. *Methods Enzymol. (in press)*
- Kriz, W., Schnermann, J., Koepsell, H. 1972. The position of short and long loops of Henle in the rat kidney. *Z. Anat. Entwickl.-Gesch.* **138**:301–319
- Lin, J.-T., Szwarc, K., Kinne, R., Jung, C.Y. 1984. Structural state of the Na<sup>+</sup>/D-glucose cotransporter in calf kidney brush-border membranes. Target size analysis of Na<sup>+</sup>-dependent phlorizin binding and Na<sup>+</sup>-dependent D-glucose transport. *Biochim. Biophys. Acta* **777**:201–208
- Mannervik, B. 1981. Design and analysis of kinetic experiments for discrimination between rival models. In: Kinetic Data Analysis. L. Endrenyi, editor. pp. 235–270. Plenum, New York
- Neeb, M., Fasold, H., Koepsell, H. 1985. Identification of the D-glucose binding polypeptide of the renal Na<sup>+</sup> D-glucose cotransporter with a covalently binding D-glucose analog. *FEBS Lett.* **182**:139–144
- Neeb, M., Kunz, U., Koepsell, H. 1987. Identification of D-glucose-binding polypeptides which are components of the renal Na<sup>+</sup>-D-glucose cotransporter. *J. Biol. Chem.* **262**:10718–10727
- Peerce, B.E., Wright, E.M. 1984. Sodium-induced conformational changes in the glucose transporter of intestinal brush borders. *J. Biol. Chem.* **259**:14105–14112
- Peerce, B.E., Wright, E.M. 1985. Evidence for tyrosyl residues at the Na<sup>+</sup> site on the intestinal Na<sup>+</sup>/glucose cotransporter. *J. Biol. Chem.* **260**:6026–6031
- Scatchard, G. 1949. The attractions of proteins for small molecules and ions. *Ann. NY Acad. Sci.* **51**:660–672
- Semenza, G., Kessler, M., Hosang, M., Weber, J., Schmidt, U. 1984. Biochemistry of the Na<sup>+</sup>, D-glucose cotransporter of the small intestinal brush-border membrane. The state of the art in 1984. *Biochim. Biophys. Acta* **779**:343–379
- Takahashi, M., Malathi, P., Preiser, H., Jung, C.Y. 1985. Radiation inactivation studies on the rabbit kidney sodium-dependent glucose transporter. *J. Biol. Chem.* **260**:10551–10556
- Toggenburger, G., Kessler, M., Rothstein, A., Semenza, G., Tannenbaum, C. 1978. Similarity in effects of Na<sup>+</sup> gradients and membrane potentials on D-glucose transport by, and phlorizin binding to, vesicles derived from brush borders of

- rabbit intestinal mucosal cells. *J. Membrane Biol.* **40**:269–290
33. Toggenburger, G., Kessler, M., Semenza, G. 1982. Phlorizin as a probe of the small-intestinal Na<sup>+</sup>,D-glucose cotransporter. A model. *Biochim. Biophys. Acta* **688**:557–571
34. Turner, R.J., Kempner, E.S. 1982. Radiation inactivation studies of the renal brush-border membrane phlorizin-binding protein. *J. Biol. Chem.* **257**:10794–10797
35. Turner, R.J., Moran, A. 1982. Further studies of proximal tubular brush border membrane D-glucose transport heterogeneity. *J. Membrane Biol.* **70**:37–45
36. Turner, R.J., Moran, A. 1982. Heterogeneity of sodium-dependent D-glucose transport sites along the proximal tubule: Evidence from vesicle studies. *Am. J. Physiol.* **242**:F406–F414
37. Turner, R.J., Moran, A. 1982. Stoichiometric studies of the renal outer cortical brush border membrane D-glucose transporter. *J. Membrane Biol.* **67**:73–80
38. Weber, W.-M., Schwarz, W., Passow, H. 1989. Endogenous D-glucose transport in oocytes of *Xenopus laevis*. *J. Membrane Biol.* **111**:93–102

Received 6 June 1989; revised 20 September 1989